# ON THE PHASE SEPARATION OF THE LIQUID SYSTEMS $Ne–H_2$ AND $Ne–D_2$





J. P. BROUWER

# ON THE PHASE SEPARATION OF THE LIQUID SYSTEMS $Ne–H_2$ AND $Ne–D_2$

# ON THE PHASE SEPARATION OF THE LIQUID SYSTEMS $Ne–H_2$ AND $Ne–D_2$



PROEFSCHRIFT

TER VERKRIJGING VAN DE GRAAD VAN DOCTOR
IN DE WISKUNDE EN NATUURWETENSCHAPPEN AAN DE
RIJKSUNIVERSITEIT TE LEIDEN,
OP GEZAG VAN DE RECTOR MAGNIFICUS DR. J. GOSLINGS,
HOOGLERAAR IN DE FACULTEIT DER GENEESKUNDE,
TEN OVERSTAAN VAN EEN COMMISSIE UIT DE SENAAT
TE VERDEDIGEN OP DONDERDAG 18 JUNI 1970
TE KLOKKE 14.15 UUR

DOOR

JAN PETER BROUWER
GEBOREN TE MAGELANG, INDONESIE IN 1938



1970
KONINKLIJKE DRUKKERIJ VAN DE GARDE N.V.
ZALTBOMMEL

Promotor: PROF. DR. K. W. TACONIS

*Dit proefschrift is tot stand gekomen onder leiding van*

PROF. DR. J. J. M. BEENAKKER en DR. C. J. N. VAN DEN MEIJDENBERG

# STELLINGEN

## I

Voor het bepalen van de faseschеidingskromme van een vloeibaar binair systeem, biedt de methode in het eerste hoofdstuk van dit proefschrift beschreven, vele voordelen boven de gebruikelijke methoden.

Wilson, J. M., Newcombe, R. J., Denaro, A. R. en Rickett, R. M. W., Experiments in Physical Chemistry (Pergamon Press Ltd. 1968).
Dit proefschrift, hoofdstuk I.

## II

Prydz heeft een empirische toestandsvergelijking voor deuterium opgesteld voor het temperatuurgebied van 20 tot 400 K, voornamelijk gebruik makend van de experimentele gegevens voor de gasfase boven 100 K. De met deze procedure gevonden waarden van de tweede viriaal-coëfficiënt beneden 50 K zijn aanvechtbaar vanwege het niet in aanmerking nemen van quantum-effecten.

Prydz, R., Nat. Bur. Std., Rept. 9276 (1967).

## III

Een meting van de drukafhankelijkheid van de kritische ontmeng-temperatuur voor het systeem Ne–$H_2$ zou belangrijke additionele informatie kunnen verschaffen over de geldigheid van de theorie van Simon en Bellemans voor mengsels van isotopen.

Simon, M. en Bellemans, A., Physica **26** (1960) 191.
Dit proefschrift, hoofdstuk III.

## IV

Bij NMR metingen in metalen waarin zowel quadrupool-effecten als Knight shift anisotropie optreden, kan het in bepaalde gevallen beter zijn de Knight shift te meten aan de quadrupool-satellieten dan aan de centrale lijn zelf.

## V

Ten onrechte suggereert Streett dat de verschillen in de faseschei dingskrommen van de systemen Ne–$D_2$ en Ne–$H_2$ voornamelijk veroorzaakt worden door verschillen in de dampspanning van $D_2$ en $H_2$.

Streett, W. B., Proc. Intern. Cryog. Eng. Conf., 2nd., Brighton, U. K. (1968) 260.

## VI

Voor de warmtegeleidingsmetingen aan He II bij 1,563 K van Brewer en Edwards kan het drukverschil over het meetcapillair als functie van de warmtestroom, verklaard worden door aan te nemen dat de stroming van het normale fluidum bij lage snelheden laminair is en bij hoge snelheden klassiek turbulent.

Brewer, D. F. en Edwards, D. O., Phil. Mag. **6** (1961) 1173.
Wilks, J., The Properties of Liquid and Solid Helium (Clarendon Press, Oxford 1967) pag. 377.

## VII

De door Dzialoshinskii opgegeven waarde voor het spontane magnetische moment van $\alpha$–$Fe_2O_3$ stemt niet overeen met de meetresultaten van Néel en Pauthenet.

Dzialoshinskii, I. E., Sov. Phys. – J.E.T.P. **5** (1957) 1259.
Néel, L. en Pauthenet, R., Compt. Rend. Acad. Sci. **234** (1952) 2172.

## VIII

Voor de bepaling van de warmtegeleidingscoëfficiënt met de hete draad methode wordt de correctie voor de niet-radiële warmtestroom veelal geschat. Dit kan echter aanleiding geven tot aanzienlijke fouten zoals blijkt uit de correcte oplossing van de warmtegeleidingsvergelijking.

Carlslaw, H. S. en Jaeger, J. C., Conduction of Heat in Solids (Oxford Univ. Press, London, 1959).
Kannuluik, W. G. en Martin, L. H., Proc. Roy. Soc. **A141** (1933) 144.

IX

Gezien de maatschappelijke stereotypering van individuen of groepen van individuen, die vanwege verstandelijke of lichamelijke handicaps niet in de gewone klassikale vormen van onderwijs zijn in te passen, behoort het tot de taak van overheid en onderwijsinstanties door deskundige informatie op dit punt een mentaliteitsverandering in de samenleving te bewerkstelligen.

X

Het gebruik van prikkeldraad als afrastering dient met name in de bebouwde kom vermeden te worden.

*Aan Marieke*

*Dit werk is een onderdeel van het programma van de Stichting voor Fundamenteel Onderzoek der Materie (F.O.M.) en is mogelijk gemaakt door financiële steun van de Nederlandse Organisatie voor Zuiver Wetenschappelijk Onderzoek (Z.W.O.).*

# CONTENTS

# INTRODUCTION

Thermodynamic properties of mixtures of simple molecules at low temperatures, both in the gaseous and liquid state have been the subject during the last decade of several experimental studies in the Kamerlingh Onnes Laboratorium[1–6]). The purpose of these studies was to determine the thermodynamic excess functions of mixtures with the aim of testing the validity of the theories of mixtures developed by the schools of Prigogine[7,8]) and Scott[9]).

A group of mixtures of special interest is formed by the liquid mixtures of light molecules, where quantum-effects play an important role. An useful measure for the influence of quantum-effects has been introduced by De Boer[10]). For a liquid made up of cells of linear dimension $\sigma$, the diameter of the molecule, the zero-point energy of a molecule is of the order of $h^2/\sigma^2 m$, where $h$ is the Planck's constant and $m$ the molecular mass. The total interaction energy of the molecule with its surrounding neighbours is in a first approximation $\frac{1}{2}z\varepsilon$, where $z$ is the number of first neighbours and $\varepsilon$ the binary interaction energy. The relative influence of the zero-point energy may thus be described by the parameter $\Lambda^{*2} = h^2/\sigma^2 m\varepsilon$.

From this it is clear that the influence of quantum effects will be large for molecules with small mass and small interaction energy. In order to study the influence of quantum effects on the properties of liquid mixtures most clearly it is appropriate to investigate mixtures of isotopes. Since for isotopes the intermolecular potentials are almost the same, departures from ideality are mainly due to the difference in quantum-effects of the pure components. Prigogine and co-workers[7]) developed a theory, relating the thermodynamic excess functions of isotopic mixtures to the zero-point energies of the pure

substances. As the calculated excess Gibbs function is found to be positive, the theory predicts that at sufficiently low temperatures phase separation occurs. For mixtures of the light isotopes $^3He$ and $^4He$ and mixtures of the hydrogen isotopes large deviations from ideality have indeed been found[1,2].

Another possibility to investigate the influence of quantum-effects is provided by the mixtures of neon and the hydrogen isotopes. Neon can be regarded as a quasi-isotope of the hydrogenic molecules because the parameters characterising the intermolecular potential of Ne are only slightly different from those of the hydrogen isotopes. Mixtures of these quasi-isotopes are especially well suited for a test of the above mentioned theory of Prigogine for the following reasons.

1) The difference in mass, and as a consequence also the difference in zero-point energy, between neon and the hydrogen isotopes is much larger than for any set of true isotopes.
2) The mixtures of neon and the hydrogen isotopes are in the liquid state at temperatures where the influence of the difference in statistics does not play a significant role.

In this thesis experiments on the liquid systems Ne–$D_2$ and Ne–$H_2$ are described. The deviations from ideal mixing are actually so large that phase separation does occur in these liquid systems.

In chapter I the visual method of establishing the phase separation of the liquid Ne–$D_2$ mixtures is described. It appears that with this method the phase diagram can be determined accurately in a simple and direct way. For a more quantitative test of the theory of isotopic mixtures, information on the excess thermodynamic quantities is necessary. Such information has been obtained from measurements on the specific heat of the liquid systems Ne–$H_2$ and Ne–$D_2$.

In chapter II the specific-heat measurements for the system Ne–$H_2$ are described. The relation between the specific heat of the liquid and the measured heat capacity of the liquid-vapour system is derived, yielding an expression for the rather complicated vapour correction. From the obtained specific heat data the thermodynamic excess functions $H^E$, $S^E$ and $G^E$ are calculated.

In chapter III the specific heat data of the system Ne–$D_2$ are given, together with the calculated values of $H^E$, $S^E$ and $G^E$ for this system. In this chapter we also discuss the behaviour of some thermodynamic quantities in the neighbourhood of the upper critical consolute point, both for the systems Ne–$H_2$ and Ne–$D_2$. Finally a comparison is made between the experimental excess functions and the excess functions calculated on the basis of Prigogine's theory for isotopic quantum mixtures.

## GENERAL REFERENCES


1) De Bruyn Ouboter, R., Thesis Leiden (1961); Physica **25** (1959) 1162; Physica **26** (1960) 853; Physica **27** (1961) 219.
2) Knaap, H. F. P., Thesis Leiden (1962); Physica **26** (1960) 43, 343, 633; Physica **27** (1961) 309, 523; Physica **28** (1962) 21.
3) Knoester, M., Thesis Leiden (1966); Physica **33** (1967) 389, 410.
4) Van Eynsbergen, B., Thesis Leiden (1966); Physica **39** (1968) 499, 519.
5) Taconis, K. W. and De Bruyn Ouboter, R., Progr. in Low Temp. Phys., ed. C. J. Gorter (North Holland Publishing Cy., Amsterdam, 1964) Vol. IV, chap. 2.
6) Beenakker, J. J. M. and Knaap, H. F. P., Progr. in Low Temp. Phys., ed. C. J. Gorter (North Holland Publishing Cy., Amsterdam, 1967) Vol. V, chap. 7.
7) Prigogine, I., The molecular theory of solutions (North Holland Publishing Cy., Amsterdam, 1957).
8) Bellemans, A., Mathot, V. and Simon, M., Adv. Chem. Phys. **11** (1967) 117.
9) Scott, R. L., J. Chem. Phys. **25** (1956) 163.
10) De Boer, J., Physica **14** (1948) 139.

CHAPTER I

# PHASE SEPARATION IN THE LIQUID MIXTURE OF NEON AND DEUTERIUM

**Synopsis**

It has been observed that a liquid mixture of Ne and $D_2$ separates into two phases. The phase-separation curve has been determined between the upper critical consolute temperature (25.8°K) and the temperature at which the phase-separation curve intersects the freezing curve (23.8°K). The phase diagram has been completed by measuring the freezing- and melting curves of the mixture.

1. *Introduction.* In recent years considerable interest has been shown in the properties of liquid and solid mixtures of isotopes [1) 2) 3) 4)]. A survey of the properties of these mixtures has been published by White and Knobler [5)]. Since Ne and $D_2$ have nearly the same potential parameters for the intermolecular interaction (see table I) one can to a certain extent regard these molecules as isotopes. Their difference in mass, however, is quite considerable and therefore is the phase separation that has been observed in the liquid mixture of Ne and $D_2$ almost entirely due to the considerable difference in zero-point energy.

TABLE I

Molecular constants for neon and deuterium [6)]

| | $\sigma$ Å | $\epsilon/k$ °K | $M$ |
|---|---|---|---|
| Ne | 2.75 | 35.6 | 20.18 |
| $D_2$ | 2.95 | 35.2 | 4.03 |

This in contrast to the properties of the $^4He-^3He$ mixtures, where the quantum statistics of the molecules also play an important role [2)]. While our work was in course Simon [7)] reported results on the vapour-liquid equilibrium of $Ne-D_2$ mixtures, which also point to a phase separation and large positive deviations from Raoult's law.

2. *Experimental method.* The apparatus used for the experiments is outlined in fig. 1. The main parts of it are the measuring vessels $V_1$, $V_2$ and $V_3$ in which the phase separation was observed. To cover the temperature

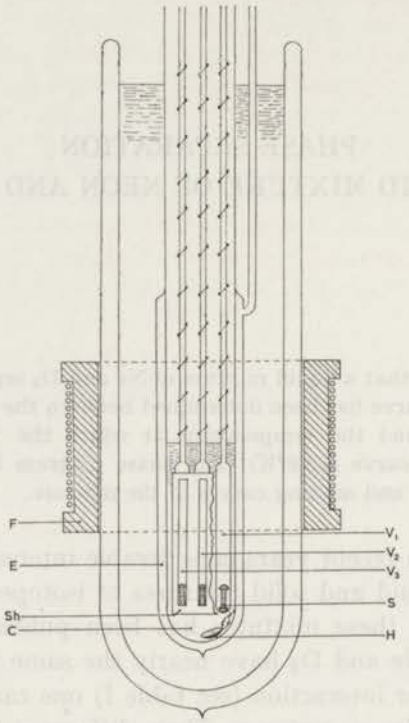


Fig. 1. Apparatus for the investigation of the phase diagram of Ne and $D_2$.

range between 18.7°K and 27°K we did not use a pressurized liquid hydrogen cryostat since the pressure necessary for the highest temperatures (5 atm) would be too high for a normal glass dewar. Therefore an extra inner cryostat $C$ was used in which Ne or $D_2$ was condensed. In this way the whole temperature range from 18.7 to 27°K could be covered without having pressures higher than 1.5 atm. The inner cryostat $C$ was surrounded by a liquid hydrogen bath, from which it could be insulated by evacuating the vacuum jacket $E$. When starting the experiment some gas is let into the vacuum jacket $E$ and the outer dewar is filled with liquid hydrogen. Subsequently about 100 liter NTP Ne or $D_2$ gas is condensed into $C$. By pumping $E$ the liquid in $C$ is isolated from the liquid hydrogen bath and can be heated to the desired temperature, which is kept constant within 0.01°K by controlling the vapour pressure of the liquid (see fig. 2). The method applied here is described in detail in an earlier publication [8]). The change in the bath pressure gives rise to a variation of the oil-level in the differential mano-

meter $M$, which causes a change in the capacitance of a condensor $C_1$. Changes in capacitance affect a circuit, which controls the current through the heater $H$ in the liquid bath $C$, whereas the necessary cooling is supplied to the vapour above the bath through the glass wall, which is directly in contact with the surrounding liquid hydrogen bath.

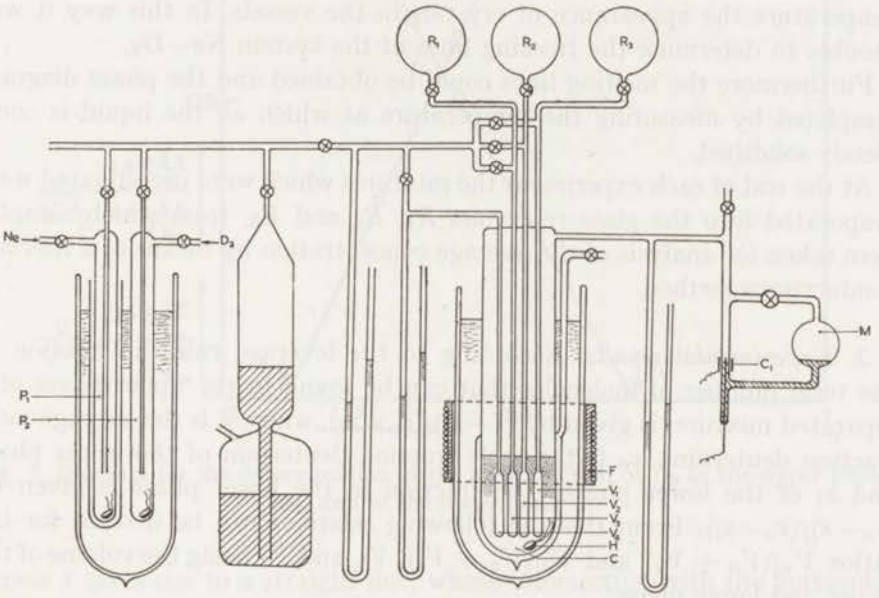


Fig. 2. A schematic diagram of the set-up.

The three measuring vessels in the inner cryostat $C$ are filled with liquid mixtures of Ne and $D_2$ of different compositions by distillation out of the purifying vessels $P_1$ and $P_2$, which are placed in a separate cryostat and which contain the pure liquid components. A fourth identical vessel $V_4$ is filled with pure Ne or $D_2$ and serves as a vapour-pressure thermometer. The four vessels are surrounded by a copper shield $Sh$ to ensure a good temperature equality between the vessels. The liquids in the vessels can be agitated with small metal stirrers $S$, operated by means of the magnetic field of a coil $F$ outside the cryostat.

The phase separation that occurs in the three vessels $V_1$, $V_2$ and $V_3$ could be observed from outside the cryostat since the whole apparatus was made of glass. In each vessel the positions of the two meniscuses were measured with a cathetometer relative to a reference mark etched on the vessels. One can calculate the volume of the upper phase $V_u$ and of the lower phase $V_l$, using the calibration of the volume of each vessel as a function of the distance from the reference mark.

In the phase-separation region the vapour pressure at one temperature

has to be independent of the concentration; and this was found to be true within 0.5%. From the vapour pressure of the pure Ne and $D_2$ in the fourth vessel the temperature at which the measurement was performed was derived, this temperature agreed within 0.03°K with the temperature derived from the vapour pressure of the surrounding liquid Ne or $D_2$ bath.

When the bath temperature in $C$ is lowered one observes at a certain temperature the appearance of crystals in the vessels. In this way it was possible to determine the freezing lines of the system Ne—$D_2$.

Furthermore the melting lines could be obtained and the phase diagram completed by measuring the temperature at which all the liquid is completely solidified.

At the end of each experiment the mixtures which were investigated were evaporated into the glass reservoirs $R_1$, $R_2$ and $R_3$, from which samples were taken for analysis of the average concentration by means of a thermal conductivity method.

3. *Experimental results.* According to the leverage rule the fraction of the total number of molecules that can be found in the upper phase of a separated mixture, is given by $(\bar{x}-x_l)/(x_u-x_l)$, where $\bar{x}$ is the average mole fraction deuterium, $x_u$ is the mole fraction deuterium of the upper phase and $x_l$ of the lower phase. The fraction in the lower phase is given by $(x_u-\bar{x})/(x_u-x_l)$. From this the following relations can be derived for the ratios $V_u/(V_u+V_l)$ and $V_l/(V_u+V_l)$, $V_u$ and $V_l$ being the volume of the upper and lower phase:

$$\frac{V_u}{V_u+V_l}\left\{\frac{1+\bar{x}\,\Delta v/v_{Ne}}{1+x_u\,\Delta v/v_{Ne}}\right\}=\frac{\bar{x}-x_l}{x_u-x_l} \tag{1a}$$

$$\frac{V_l}{V_u+V_l}\left\{\frac{1+\bar{x}\,\Delta v/v_{Ne}}{1+x_l\,\Delta v/v_{Ne}}\right\}=\frac{x_u-\bar{x}}{x_u-x_l}. \tag{1b}$$

Here $v_{Ne}$ is the molar volume of neon and $\Delta v$ the difference in molar volume between $D_2$ and Ne. In these formulae the volume change of mixing has been neglected, since even a rather large volume change of mixing of 1%, gives a correction term to the above formulae only of the order of 0.1%. From each measurement at a given temperature we obtained three values of $V_u/(V_u+V_l)$ and $V_l/(V_u+V_l)$ corresponding to three differently chosen filling compositions $\bar{x}$. Using these values and introducing a trial value for $x_u$ to determine the term between the brackets, which gives a correction of about 20%, one can calculate the left-hand side of formula (1$a$). It is obvious from formula (1$a$) that a plot of the quantity

$$\frac{V_u}{V_u+V_l}\left\{\frac{1+\bar{x}\,\Delta v/v_{Ne}}{1+x_u\,\Delta v/v_{Ne}}\right\}$$

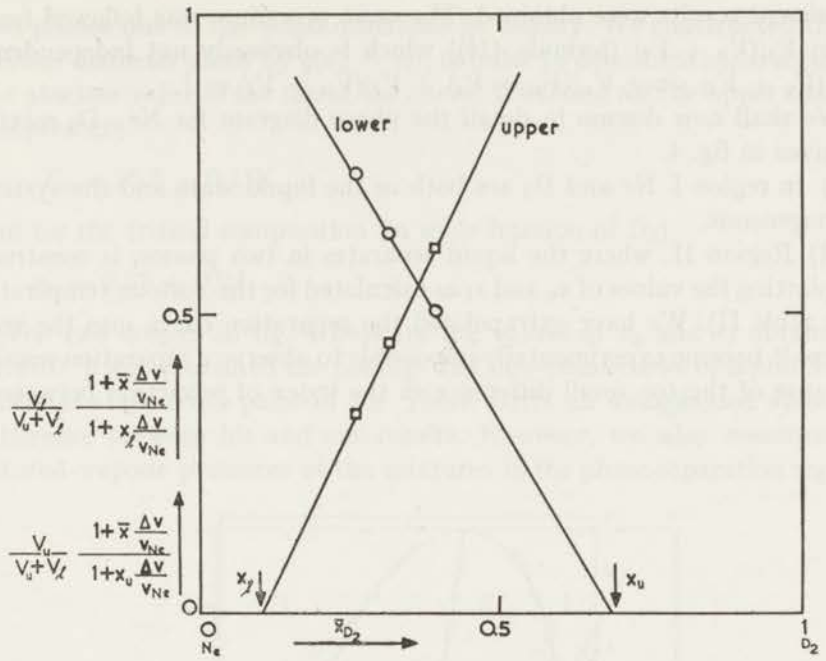


Fig. 3. Diagram for the determination of the mole fraction of $D_2$ in the upper phase, $x_u$, and in the lower phase $x_l$.

versus $\bar{x}$ gives rise to a straight line, whose intersection with the horizontal axis is $x_l$ and whose slope is given by $1/(x_u - x_l)$. As can be seen from fig. 3 the three points lie rather well on a straight line, so that $x_l$ and $x_u$ can be read off accurately. In the cases when the values for $x_u$ and $x_l$ did not agree with the trial value, a successive approximation procedure was followed till

TABLE II

Results of the measurements in the phase-separation region

| $T$ °K | $x_l$ mole fraction $D_2$ in lower phase | $x_u$ mole fraction $D_2$ in upper phase | $p$ cm Hg |
|---|---|---|---|
| 25.60 | 0.216 | 0.500 | 151.75 |
| 25.51 | 0.195 | 0.525 | |
| 25.39 | 0.185 | 0.545 | 143.99 |
| 25.17 | 0.164 | 0.589 | 135.93 |
| 24.91 | 0.125 | 0.650 | 127.51 |
| 24.85 | 0.118 | 0.648 | 125.08 |
| 24.83 | 0.129 | 0.645 | 123.71 |
| 24.75 | 0.120 | 0.658 | |
| 24.72 | 0.127 | 0.665 | |
| 24.41 | 0.112 | 0.700 | 110.51 |
| 24.11 | 0.100 | 0.730 | 102.27 |
| 23.91 | 0.095 | 0.738 | 97.33 |

consistent results were obtained. The same procedure was followed for the ratio $V_l/(V_u + V_l)$ (formula (1b)) which is obviously not independent of $V_u/(V_u + V_l)$ since $V_u/(V_u + V_l) + V_l/(V_u + V_l) = 1$.

We shall now discuss in detail the phase diagram for $Ne-D_2$ mixtures as given in fig. 4.

I) In region I Ne and $D_2$ are both in the liquid state and the system is homogeneous.

II) Region II, where the liquid separates in two phases, is constructed by plotting the values of $x_u$ and $x_l$ as calculated for the various temperatures (see table II). We have extrapolated the separation curve into the region where it became experimentally impossible to observe a separation meniscus because of the too small difference in the index of refraction between the

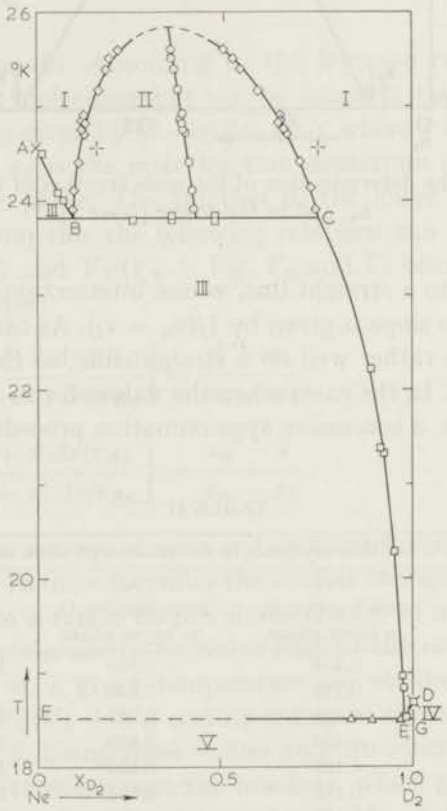


Fig. 4. The phase diagram for the $Ne-D_2$ mixture.

◇ $x_u$ and $x_l$
○ $(x_u + x_l)/2$
□ freezing points
△ melting points
× triple points of the pure components [10] [11]
+ $x_u$ and $x_l$, Simon [7].

two phases due to the small difference in density. We constructed the rectilinear diameter given by $\frac{1}{2}(x_u + x_l)$, in order to determine more accurately the abscissa value of the top of the curve. We found for the upper consolute temperature

$$T_c = 25.8 \pm 0.1°K$$

and for the critical composition (in mole fraction of $D_2$)

$$x_c = 0.35 \pm 0.02.$$

The two crosses in fig. 4 indicate the values of $x_u$ and $x_l$ obtained by Simon [7]) who measured the boiling- and dew-point curve of liquid Ne—$D_2$ mixtures at the triple point of Ne. There exists an unexplained systematic difference between his and our results. However, we also measured the satured vapour pressures of the mixtures in the phase-separation region at

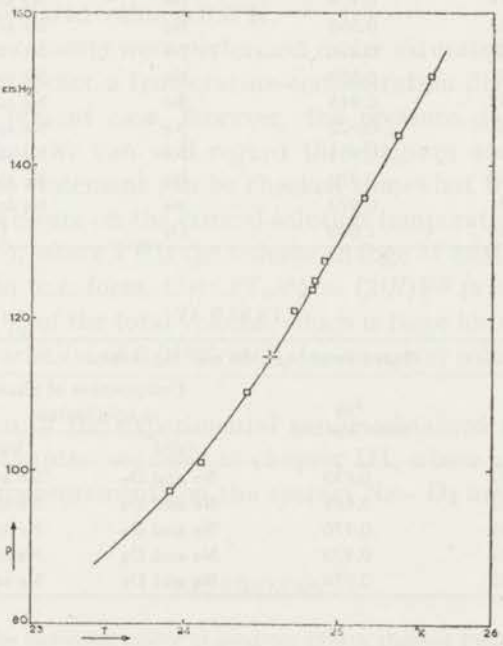


Fig. 5. Vapour pressure as a function of the temperature in the phase-separation region
+ Simon [7]) □ this research.

various temperatures. The vapour pressure measured by Simon at 24.57°K agrees very well with our results as can be seen from fig. 5.

The boundary *BC* between the phase-separation region II and the liquid solid region III, was measured by observing the temperature at which the first crystals appeared in the separated mixture.

III) In region III pure solid Ne-crystals are in equilibrium with a liquid

mixture of Ne and $D_2$. The lines $AB$ and $CE$ are constructed by plotting the measured freezing-point temperatures versus the concentration (see table III). The boundary $FE$ between region III and region V was given by the temperature at which the mixture completely solidified (see table IV). The eutectic point was found to be 18.5[2] °K.

TABLE III

| Measurements of the freezing points | | | |
|---|---|---|---|
| $T$ °K | $x_{D_2}$ mole fraction | Composition of phases in equilibrium | |
| | | solid | liquid |
| 24.50 | 0.012 | Ne | Ne and $D_2$ |
| 24.05 | 0.054 | Ne | Ne and $D_2$ |
| 23.97 | 0.069 | Ne | Ne and $D_2$ |
| 23.79 | 0.253 | Ne | Ne and $D_2$ |
| 23.79 | 0.358 | Ne | Ne and $D_2$ |
| 23.79 | 0.474 | Ne | Ne and $D_2$ |
| 23.83 | 0.358 | Ne | Ne and $D_2$ |
| 23.83 | 0.474 | Ne | Ne and $D_2$ |
| 22.22 | 0.889 | Ne | Ne and $D_2$ |
| 21.37 | 0.915 | Ne | Ne and $D_2$ |
| 21.34 | 0.922 | Ne | Ne and $D_2$ |
| 20.28 | 0.951 | Ne | Ne and $D_2$ |
| 18.96 | 0.970 | Ne | Ne and $D_2$ |
| 18.84 | 0.973 | Ne | Ne and $D_2$ |
| 18.68 | 1.000 | $D_2$ | $D_2$ |

TABLE IV

| Measurements of the melting points | | | |
|---|---|---|---|
| $T$ °K | $x_{D_2}$ mole fraction | Composition of phases in equilibrium | |
| | | solid | liquid |
| 18.52 | 0.833 | Ne and $D_2$ | Ne and $D_2$ |
| 18.52 | 0.889 | Ne and $D_2$ | Ne and $D_2$ |
| 18.52 | 0.970 | Ne and $D_2$ | Ne and $D_2$ |
| 18.52 | 0.973 | Ne and $D_2$ | Ne and $D_2$ |
| 18.52 | 0.978 | Ne and $D_2$ | Ne and $D_2$ |

IV) Likewise in region IV pure solid $D_2$ is in equilibrium with a liquid Ne—$D_2$ mixture, the composition of which is given by line $DE$. This region turned out to be very small.

V) In region V the whole system is solid.

A diagram similar to the one we investigated has been extensively discussed by Vogel [9]).

As can be seen from the picture the measured lines $AB$ and $DE$ extrapolate well (within 0.01°K) to the triple-point temperatures $A$ and $D$ of the pure components as found in the literature [10]) [11]). The lowering of the

freezing point $\Delta T$ for the point $B$ where the freezing curve meets the phase-separation curve, amounts 0.8°K, whereas we calculated a freezing-point lowering of 1.1°K using the formula:

$$\Delta T = T\{RT \ln (1 - x) + wx^2\}/\Delta Q \qquad (2)$$

where $\Delta Q$ is the latent heat of fusion of the pure component. The influence of the non-ideality of the mixture was estimated by introducing a term $wx^2$; this is valid for a regular solution. In this case the value of $w$ is connected with the upper consolute temperature by:

$$T_c = w/2R = (2/R)G^E(x = 0.5) \qquad (3)$$

which makes $wx^2$ a correction term of 10%. Since the shape of the phase-separation curve is not symmetric in our case, the solution is clearly not regular, but we can use the formula for regular solutions as an approximation.

At the pure deuterium side the experimental freezing-point lowering is 0.2°K and the calculated value is 0.3°K.

Since our measurements were performed under saturated vapour pressure the phase diagram is not a temperature-concentration diagram at constant pressure. In the present case, however, the pressure did not vary more than 1 atm so that we can still regard the diagram as a constant-pressure diagram. This statement can be checked somewhat by considering the influence of the pressure on the critical solution temperature which is given by $\partial G^E/\partial p = V^E$ [1]), where $V^E$ is the volume change of mixing. For a regular mixture we obtain (c.f. form. (3)): $\partial T_c/\partial p = (2/R)V^E\ (x = 0.5)$. Assuming a value of $V^E$ of 1% of the total volume, which is large for this kind of molecules, we find a variation of 0.01°K in $T_c$ for a regular solution.

For a discussion of the experimental results obtained with the method described in this chapter, we refer to chapter III, where also the results of the specific heat measurements on the system $Ne-D_2$ are given.

REFERENCES


1) Prigogine, I., The molecular theory of solutions (North Holland Publishing Company, Amsterdam, 1957).
2) De Bruyn Ouboter, R., Beenakker, J. J. M. and Taconis, K. W., Communications Kamerlingh Onnes Lab., Leiden Suppl. No. 116*c*; Physica **25** (1959) 1162, Commun. Leiden No. 324*b*; Physica **26** (1960) 853 and Commun. Leiden Suppl. No. 119*a*; Physica **27** (1961) 219.
3) Knaap, H. F. P., Knoester, M. and Beenakker, J. J. M., Commun. Leiden No. 325*c*; Physica **27** (1961) 309.
4) Knaap, H. F. P., Van Heyningen, R. J. J., Korving, J. and Beenakker, J. J. M., Commun. Leiden No. 333*b*; Physica **28** (1962) 343.
5) White, D. and Knobler, C. M., An. Rev. phys. Chem. **14** (1963) 251.
6) Hirschfelder, J. O., Curtiss, C. F. and Bird, R. B., Molecular theory of gases and liquids (John Wiley, New York, 1954); Michels, A., De Graaff, W. and Ten Seldam, C. A., Physica **26** (1960) 393.

7) Simon, M., Physics Letters **2** (1962) 234 and Physica **29** (1963) 1079.
8) Coremans, J. M. J., Van Itterbeek, A., Beenakker, J. J. M., Knaap, H. F. P. and Zandbergen, P., Commun. Leiden No. 311*a*; Physica **24** (1958) 557.
9) Vogel, D., Die heterogenen Gleichgewichte (Handbuch der Metallphysik, Vol. II, p. 161, p. 220, Leipzig, 1937).
10) Henning, F. and Otto, J., Phys. Z. **37** (1936) 633.
11) Woolley, H. W., Scott, R. B. and Brickwedde, F. G., J. Res. Nat. Bur. Stand. **41** (1948) 379.

CHAPTER II

# SPECIFIC HEAT OF THE LIQUID MIXTURES OF NEON AND HYDROGEN ISOTOPES IN THE PHASE-SEPARATION REGION

## THE SYSTEM Ne–$H_2$

**Synopsis**

The phase separation in the liquid binary system of neon and normal hydrogen has been investigated by measuring the specific heat at saturation for different compositions between 24 K and 30 K. The phase-separation curve has been determined. The coordinates of the upper critical consolute point are $T_c = 28.93$ K and $x_{H_2} = 0.308$. The temperature at which the liquid phase-separation curve meets the freezing curve is $T_M = 24.27$ K. The excess enthalpy, the excess entropy and the excess Gibbs function of the liquid mixture have been calculated as functions of temperature and composition. The vapour correction for heat-capacity measurements of a two component liquid-vapour system is discussed.

1. *Introduction.* Departures from classical behaviour have been investigated for several mixtures of isotopes[1,2,3,4]). These deviations are significant when the zero-point energy of a molecule in the liquid cannot be neglected in comparison with the interaction energy of the molecule with its surrounding neighbours. The relative influence of the zero-point energy in a pure substance can be described with the dimensionless parameter $\Lambda^* = h/\sigma(m\varepsilon)^{\frac{1}{2}}$ [5]), where $h$ is the Planck's constant, $m$ the molecular mass and $\sigma$ and $\varepsilon$ the potential parameters of the binary interaction between the molecules. From this it is clear that liquid mixtures containing molecules of small mass and small interaction energy will also show quantum effects. Prigogine *et al.*[6]) developed a theory relating the thermodynamic excess functions of liquid isotopic mixtures to the zero-point energy. Since both $\sigma$ and $\varepsilon$ are approximately equal for isotopes, the difference in $\Lambda^*$ is the main cause for the occurrence of an excess in the thermodynamic functions. For

mixtures of $^3$He and $^4$He the picture is more complicated, since the temperature at which this system becomes liquid is so low that the difference in statistics of the two components also is of importance.

The most appropriate systems to study the influence of zero-point energy are therefore those containing the isotopes of hydrogen. For a survey of the available thermodynamic data on the liquid mixtures of the hydrogen isotopes we refer to ref. 7. A comparison of theory and experiment for these isotopic mixtures indeed leads to a reasonable agreement.

TABLE I

Molecular constants for neon and hydrogen isotopes

| | $\sigma$ (Å) | $\varepsilon/k$ (K) | $M$ | $\Lambda^*$ |
|---|---|---|---|---|
| | Lennard–Jones 6–12 | | | |
| Ne [8]) | 2.75 | 35.6 | 20.18 | 0.59 |
| $H_2$ [9]) | 2.96 | 36.7 | 2.02 | 1.73 |
| $D_2$ [9]) | 2.95 | 35.2 | 4.03 | 1.23 |

Since neon and the hydrogen isotopes have nearly the same potential parameters (see table I) one may expect that the liquid mixtures of neon and the hydrogen isotopes also show the characteristic behaviour of an isotopic mixture with large quantum effects. The validity of such a consideration has been confirmed insofar as the phase separation for mixtures of neon and the hydrogen isotopes, predicted on the basis of the theory for isotopic mixtures, has indeed been observed (chapter I) [10,11,12,13]). For a more quantitative verification of the theory for these mixtures, however, it is appropriate to make a direct comparison between the experimental and theoretical excess functions. Experimentally the most relevant excesss quantities can be derived from a measurement of the pressure-composition diagram of the liquid-vapour equilibrium or from specific heat measurements, while measurements on the heat of mixing only yield the excess enthalpy. From the pressure-composition data the excess Gibbs function is easily obtained, but to arrive at reliable values for the excess entropy and thus for the excess enthalpy very accurate data at different temperatures are required. From specific-heat measurements in the phase-separation region the excess enthalpy and excess entropy can directly be derived and the excess Gibbs function is then obtained from the difference of $H^E$ and $TS^E$.

For the systems Ne–$D_2$ and Ne–$H_2$ pressure-composition data have been published by Simon [10]), Streett and Jones [12]) and Heck and Barrick [13]). In this chapter specific-heat data on the system Ne–$H_2$ will be presented and in chapter III those on the system Ne–$D_2$. A comparison of theory and experiment for both systems will be included in the following chapter, and

there special attention will also be given to the phenomena occurring in the neighbourhood of the upper critical consolute point.

In section 2 of this chapter the calorimeter and experimental method to measure the specific heat are described. In section 3 the calculation of the vapour correction which has to be applied to the heat capacity of the two component liquid–vapour system in order to obtain the specific heat of the liquid, is discussed. In section 4 the specific-heat data obtained for the pure components and for the liquid mixture are presented, together with the derived phase diagram. In section 5 the calculation of the excess functions from the specific heat is given. The value of the excess Gibbs function is compared with $G^E$ obtained from the data on the vapour–liquid equilibrium of Streett[12]). In the appendix the thermodynamic expression for the heat capacity of a two component liquid-vapour system is derived. This expression has been used to evaluate the vapour correction.

In this work the following definitions and symbols will be used:

$R$ = gas constant
$T$ = absolute temperature
$N$ = number of moles
$x$ = mole fraction of the lighter component
$\bar{x}$ = mean mole fraction of the lighter component in a separated liquid
$\langle x \rangle$ = mean mole fraction of the whole system
$S$ = molar entropy
$H$ = molar enthalpy
$G$ = molar Gibbs function
$F$ = molar free energy
$\mu$ = chemical potential
$V$ = molar volume
$p$ = pressure
$C$ = heat capacity
$c$ = molar specific heat
$B$ = second virial coefficient

*Subscripts*

$i, j$ = species $i, j$
$l$ = lower phase of a separated liquid
$u$ = upper phase of a separated liquid
$p$ = at constant pressure
$\sigma$ = along the saturated vapour-pressure line (at saturation)
t = filling tube

*Superscripts*

G = gas phase
L = liquid phase
0 = pure substance
E = excess quantity
M = mixture
tot = total in the apparatus

The script symbols $\mathscr{S}^E$, $\mathscr{H}^E$ and normal symbols $S^E$, $H^E$ used for the excess functions, refer to a slight difference in definition of these quantities (see section 5).

2. *Apparatus and experimental method.* A schematic diagram of the apparatus used in the experiment is shown in fig. 1. The calorimeter C is a cylindrical copper container with a germanium resistance thermometer $T_1$

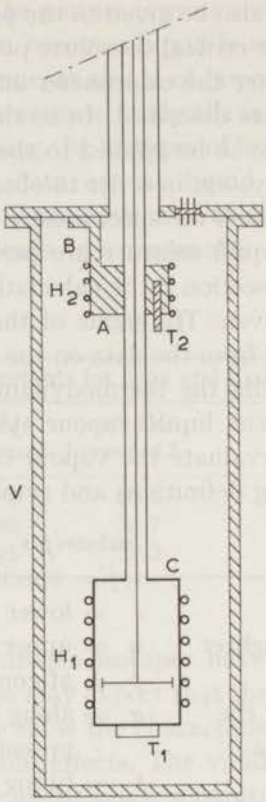

Fig. 1. The calorimeter.

attached to the bottom of the calorimeter and a heater $H_1$ wound on the outside of the cylinder. Calorimeter and filling tube are surrounded by a vacuum jacket V, and the whole apparatus is immersed in a liquid-hydrogen bath. The stirrer is connected to a rod leading through the center of the filling tube to a feed-through at the top of the cryostat so that the stirrer can be operated from outside. Both stirring rod and filling tube give rise to a considerable heat leak from the top of the cryostat, which must be reduced to avoid too large a temperature drift of the calorimeter. Therefore the filling tube is thermally connected to the hydrogen bath by the heat link B, about 10 cm above the top of the calorimeter. The temperature of the filling tube at this point A, and thus the heat exchange with the bath, can be varied by means of the heater $H_2$. The temperature of the filling tube at A is measured by the carbon thermometer $T_2$. For measurements below 20 K the bath pressure is reduced, whereas for measurements at higher temperatures the bath is kept constant at the normal boiling point of liquid hydrogen. The calorimeter is cooled down by using He as an exchange gas in the jacket and the gas is removed after the calorimeter has been charged.

The charge of the calorimeter is determined afterwards by evaporating the liquid into a calibrated glass vessel and its composition analysed by measuring the thermal conductivity of the gas mixture. For some samples the composition has also been determined by a mass-spectrometer analysis. The results of the mass-spectrometer analysis agree with the results of the thermal conductivity analysis. The total fraction of impurities in the mixtures, mainly air, never exceeded 0.005.

From the mass-spectrometer analysis the isotopic composition of the neon used in our experiments has been found to be 90.53% $^{20}$Ne, 0.33% $^{21}$Ne and 9.14% $^{22}$Ne. The amount of He (or $D_2$) and HD in the hydrogen we used has been found to be 0.20% He and 0.05% HD.

The specific-heat measurements of the mixtures have been performed using neon and normal hydrogen, *i.e.* hydrogen with the high-temperature equilibrium composition (75% ortho $H_2$ and 25% para $H_2$). That no conversion occurred during the experiment has been checked by comparing the vapour pressure of an amount of liquid normal hydrogen with the vapour pressure of 20.4 K-equilibrium hydrogen (99.8% para $H_2$ and 0.2% ortho $H_2$), both before and after it was kept in the calorimeter for several hours.

The thermometer $T_1$ has been calibrated between 15 K and 23 K against the vapour pressure of 20.4 K-equilibrium hydrogen using the International Practical Temperature Scale of 1968 (IPTS-68)[14]. Between 24.6 K and 31 K the thermometer has been calibrated against the vapour pressure of neon as measured by Grilly[15]). These data of neon have been adjusted to the IPTS-68. Furthermore a correction has been applied for the small difference in isotopic composition of our neon and the neon of ref. 15[16]).

The heat capacity of the vapour-liquid system has been determined by means of a standard calorimeter technique. The temperature of the nearly isolated calorimeter is increased by supplying a known amount of heat. The temperature increment corresponding to this energy input is obtained by extrapolation of the temperature drift before and after the heating period (see fig. 2) to the mid-time of the heating interval. The temperature change is determined with the resistance thermometer $T_1$. The resistance is measured in a wheatstone bridge, using a chart recorder as zero instrument. The typical recorder trace as given in fig. 2 shows the various steps constituting a single measuring cycle. At the beginning of the cycle the temperature at the heatlink is adjusted so as to yield approximately zero temperature drift of the calorimeter. The temperature at the heatlink is then kept constant at this value during the whole cycle. In this way the temperature $T_2$ is always a few degrees above the temperature of the calorimeter.

In the time interval from $t_1$ to $t_3$ heat is supplied, while at the end of the heating period at $t_2$ the liquid in the calorimeter is stirred a known number of times to secure equilibrium conditions in the system. During the after-

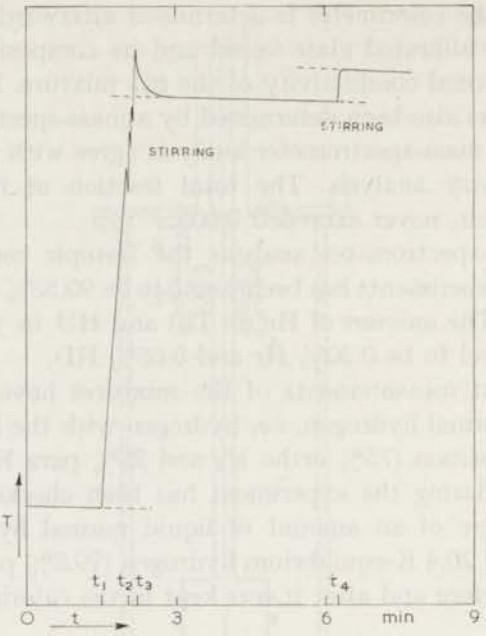


Fig. 2 Typical recorder trace.

drift at $t_4$ the liquid in the calorimeter is stirred again to calibrate the heat input due to the stirring. In order to obtain as good a calibration as possible the stirring was performed in the same way as during the heating period, but a much greater number of stirs was applied. A complete cycle also included a check of the zeropoint of the bridge by switching off the voltage over the bridge and a determination of the sensitivity of the bridge.

The charge of the calorimeter was always choosen so that the expanding liquid did not overfill the calorimeter even at the highest temperature of the run. Hence the pressure in the calorimeter was always equal to the equilibrium pressure of the liquid-vapour system at the temperature of the calorimeter.

The low-temperature volume of the calorimeter was found to be $10.20 \pm 0.05$ $cm^3$. It was found that the volume change of the calorimeter due to the temperature and pressure variation during the experiment had no influence on the heat capacity of the system.

The heat capacity of the empty calorimeter has been measured between 15 K and 30 K, and its contribution to the total heat capacity (never more than 5%) has been subtracted from the total heat capacity to obtain the heat capacity of the liquid-vapour system.

3. *The calculation of the vapour correction.* If a calorimeter contains a liquid mixture with an appreciable vapour phase the liquid will partially vapourize when the calorimeter is heated, and as a consequence the liquid

as well as the vapour will change in volume, density and composition. To obtain the specific heat of the liquid from the heat capacity of the system a rather complicated „vapour correction" has to be applied. As will be shown in the appendix the heat capacity of the calorimeter content is given by the following expression (A.14):

$$
\begin{aligned}
C = {} & N^{\mathrm{L}} c_{\sigma}^{\mathrm{L}} - N^{\mathrm{L}} T \left( \frac{\partial V^{\mathrm{L}}}{\partial T} \right)_{x^{\mathrm{L}}, p} \left( \frac{\partial p}{\partial x^{\mathrm{L}}} \right)_{T} \frac{\mathrm{d}x^{\mathrm{L}}}{\mathrm{d}T} \\
& + N^{\mathrm{G}} \left\{ c_{p}^{\mathrm{G}} - T \left( \frac{\partial V^{\mathrm{G}}}{\partial T} \right)_{x^{\mathrm{G}}, p} \frac{\mathrm{d}p}{\mathrm{d}T} \right\} \\
& - \left( \Delta_{\mathrm{e}} H_{1}^{0} - RT \ln \frac{p}{p_{1}^{0}} \right) \frac{\mathrm{d}N^{\mathrm{L}} x^{\mathrm{L}}}{\mathrm{d}T} \\
& - \left( \Delta_{\mathrm{e}} H_{2}^{0} - RT \ln \frac{p}{p_{2}^{0}} \right) \frac{\mathrm{d}N^{\mathrm{L}} (1 - x^{\mathrm{L}})}{\mathrm{d}T} \\
& + T \left( \mathscr{S}^{\mathrm{mixing, L}} - \mathscr{S}^{\mathrm{mixing, G}} \right) \frac{\mathrm{d}N^{\mathrm{L}}}{\mathrm{d}T} \\
& + TN^{\mathrm{L}} \left( \frac{\partial \mathscr{S}^{\mathrm{mixing, L}}}{\partial x^{\mathrm{L}}} \right)_{p, T} \frac{\mathrm{d}x^{\mathrm{L}}}{\mathrm{d}T} + TN^{\mathrm{G}} \left( \frac{\partial \mathscr{S}^{\mathrm{mixing, G}}}{\partial x^{\mathrm{G}}} \right)_{p, T} \frac{\mathrm{d}x^{\mathrm{G}}}{\mathrm{d}T}.
\end{aligned}
\tag{A.14}
$$

The first term in this expression represents the heat capacity of the liquid at saturation and at constant liquid composition. All the other terms constitute the vapour correction.

To evaluate the vapour corrections for the heat-capacity data obtained with each calorimeter charge, the various parts of eq. (A.14) have been calculated at integral temperatures between 24 K and 30 K. As the total vapour correction was in the order of 8% of the heat capacity of the system, we aimed for not more than 5% accuracy in these corrections. Therefore the following approximations in eq. (A.14) could be applied:

1. $N^{\mathrm{L}} T \left( \frac{\partial V^{\mathrm{L}}}{\partial T} \right)_{x^{\mathrm{L}}, p} \left( \frac{\partial p}{\partial x^{\mathrm{L}}} \right)_{T} \frac{\mathrm{d}x^{\mathrm{L}}}{\mathrm{d}T} = 0;$

2. $c_{p}^{\mathrm{G}} - T \left( \frac{\partial V^{\mathrm{G}}}{\partial T} \right)_{x^{\mathrm{G}}, p} = x^{\mathrm{G}} c_{p,1}^{0} + (1 - x^{\mathrm{G}}) c_{p,2}^{0} - V^{\mathrm{G}} \frac{\mathrm{d}p}{\mathrm{d}T};$

3. $\mathscr{S}^{\mathrm{E, G}} = 0.$

From the dimensions of the apparatus, the properties of the pure components[15,17,18,19]) and the liquid–vapour equilibrium data of the system Ne–n$H_2$[12]) the distribution of moles between liquid and gas phase has been calculated. In this calculation the excess volumes of liquid and gas phase have been neglected because it was found that a rather large excess volume

of 1% in the gas phase and of 3% in the liquid phase did not significantly influence the corrections. The composition of the liquid has been calculated starting from the average composition over liquid and gas and applying successive approximations using the liquid-vapour composition diagram as given in ref. 12. Once knowing $N^{G}(T)$, $N^{L}(T)$, $x^{L}(T)$, $x^{G}(T)$ and $p(T)$ we calculated the specific heat of the liquid from eq. (A.14) except for the small corrections involving $\mathscr{S}^{E,L}$. These latter corrections have been evaluated by calculating $\mathscr{S}^{E,L}$ in a successive approximation from the specific heat of the liquid (see section 5).

4. *The experimental results.* a. The specific heat of $pH_2$. Since accurate values of the specific heat of para hydrogen were available from measurements of Younglove and Diller[20]), we measured the specific heat of liquid $pH_2$ between 18 K and 30 K to check the experimental method. The results of these measurements are given in fig. 3. The full drawn curve represents the smoothed values of our data, whereas the points represent the values of ref. 20. Our measurements have been done with three different charges in the calorimeter and the vapour corrections have been calculated using eq. (A.14) with $x^{L} = x^{G} = 1$. Although the magnitude of the corrections were quite different for the various runs, the resulting specific-heat data coincide within the scattering of each run. Fig. 4 shows the deviations of

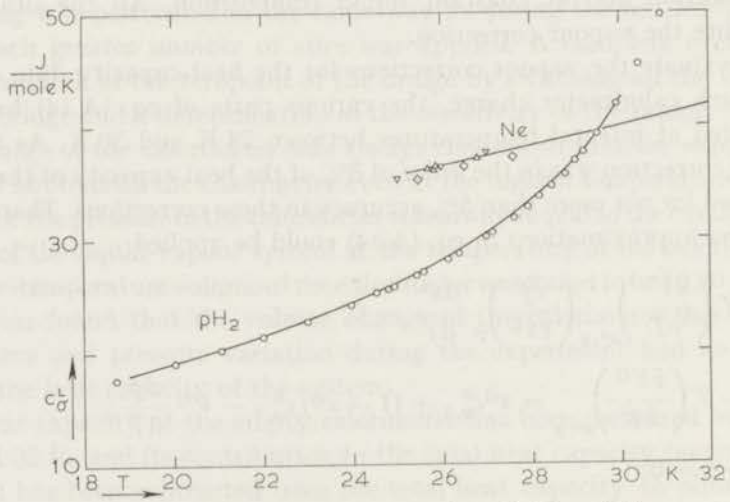


Fig. 3. The specific heat at saturation of $pH_2$ and Ne.
——— smoothed values of the present research;
○ $pH_2$, Younglove and Diller[20]);
△ Ne, Clusius[21]);
◇ Ne, Fagerstroem and Hollis–Hallett[22]);
▽ Ne, Clusius *et al.* (smoothed values)[23]).

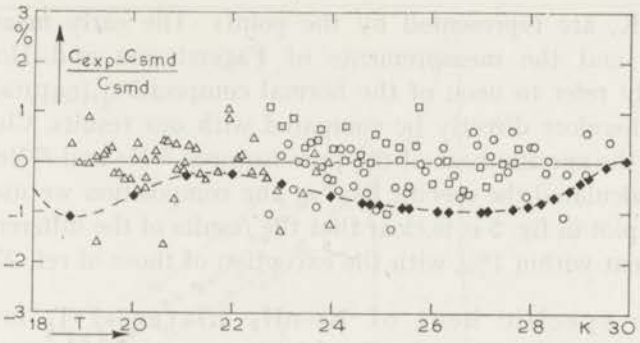


Fig. 4. Deviations of the measured specific heat of $pH_2$ from the smoothed values of the present research.
△ run 1; ○ run 2; □ run 3;
♦ Younglove and Diller[20].

all points from the smoothed curve for $pH_2$ represented in fig. 3. The typical scattering is found to be 2%. The main cause of the scattering in our results is the inaccurate reproducibility of the heat input due to the stirring. The points of Younglove and Diller in fig. 4 have been converted to the IPTS-68. Although the deviations from our smoothed values are within the limits of our accuracy, there is a clear indication that the specific-heat values of Younglove and Diller are systematically ½%–1% lower than our values.

4b. The specific heat of neon. The specific heat of neon has been measured in the temperature range from 26 K to 32 K. The full-drawn curve shown in fig. 3 represents the smoothed values obtained from our measurements. The literature data, which cover only the temperature range

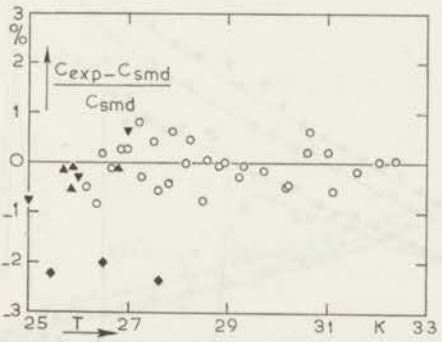


Fig. 5. Deviations of the measured specific heat of Ne from the smoothed values of the present research.
○ this research;
▲ Clusius[21];
♦ Fagerstroem and Hollis-Halett[22];
▼ Clusius *et al.* (smoothed values)[23]

up to 28 K, are represented by the points. The early measurements of Clusius[21]) and the measurements of Fagerstroem and Hollis–Hallit[22]) presumably refer to neon of the normal composition (natural abundance) and can therefore directly be compared with our results. Clusius *et al.*[23]) measured the specific heat of the pure isotopes $^{20}$Ne and $^{22}$Ne. From these data we calculated the specific heat at the composition we used. From the deviation plot in fig. 5 it is clear that the results of the different sources are in agreement within 1%, with the exception of those of ref. 22.

4c. The specific heat of Ne–n$H_2$ mixtures. To investigate the liquid mixtures of neon and normal hydrogen, specific-heat measurements have been performed for 12 mixtures of different composition. The results are given in figs. 6, 7 and 8, while in table II the smoothed specific-heat values at 0.5 K intervals are given. The two transitions appearing in most of the specific-heat curves between 24 K and 29 K can be explained on the basis of the phase diagram in fig. 9. The first sharp drop in the specific heat (at the melting temperature $T_M = 24.27$ K) determines the boundary between the liquid-solid region and the phase-separation region II (line BC in fig. 9). The second transition occurs for the various mixtures at different

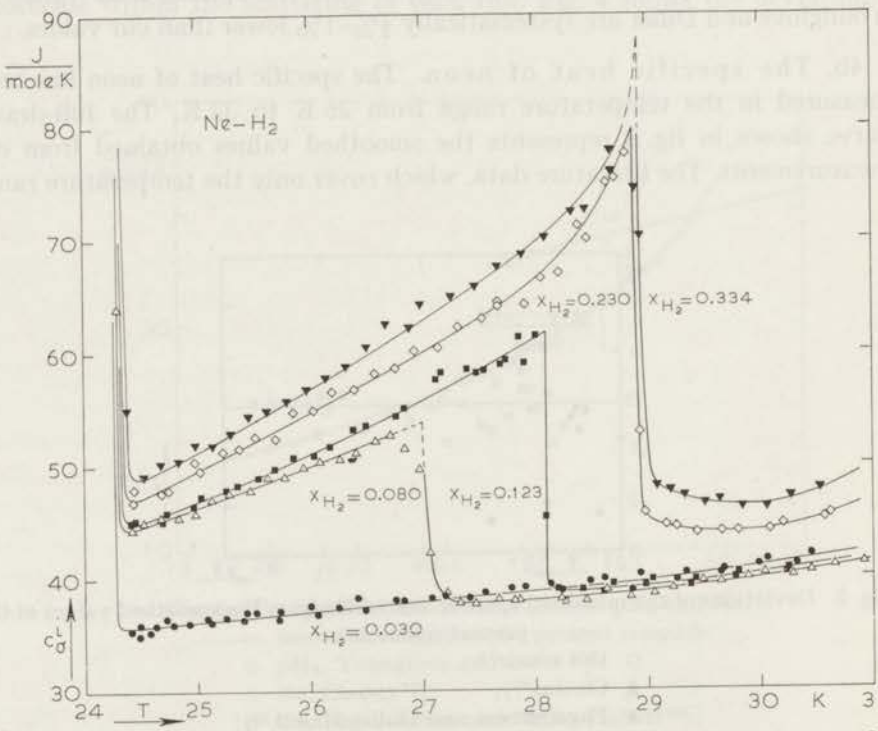


Fig. 6. Specific heat at saturation for the system Ne–$H_2$, for compositions $x_{H_2} < 0.4$.

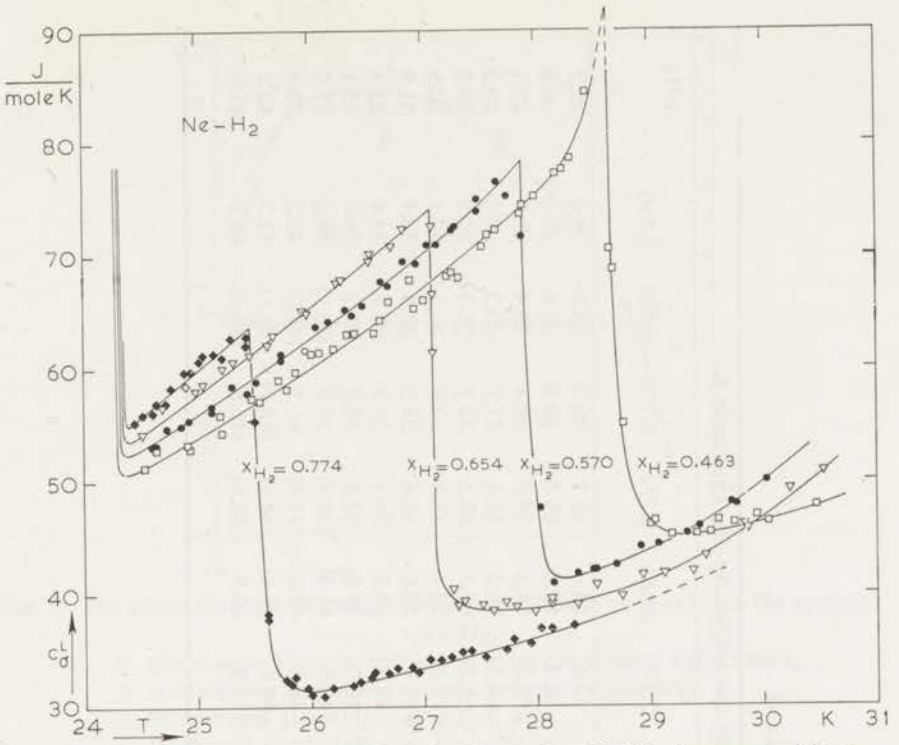


Fig. 7. Specific heat at saturation for the system Ne–$H_2$, for compositions $0.4 < x_{H_2} < 0.775$.

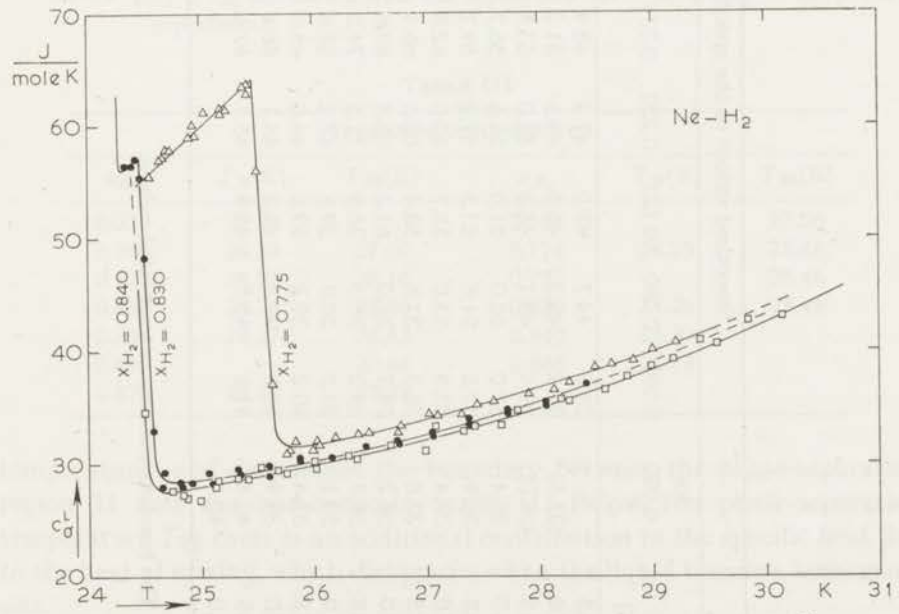


Fig. 8. Specific heat at saturation for the system Ne–$H_2$, for compositions $0.775 \leq x_{H_2}$

TABLE II

Smoothed values of the specific heat for the system Ne–$H_2$, $c_\sigma^L$(J/mole K)

| $x_{H_2}$ / $T$(K) | Ne 0.000 | 0.030 | 0.080 | 0.123 | 0.230 | 0.334 | 0.463 | 0.570 | 0.654 | 0.774 | 0.775 | 0.830 | 0.840 | $pH_2$ |
|---|---|---|---|---|---|---|---|---|---|---|---|---|---|---|
| 24.5 | | 35.8 | 44.7 | 45.0 | 47.2 | 48.9 | 51.1 | 52.8 | 54.0 | 55.7 | 55.3 | 51.0 | 36.0 | 25.3 |
| 25.0 | (35.5)* | 36.2 | 46.3 | 46.8 | 49.6 | 51.2 | 53.9 | 55.9 | 57.5 | 59.8 | 59.8 | 28.6 | 28.0 | 26.2 |
| 25.5 | (36.0) | 36.6 | 48.1 | 48.8 | 52.0 | 53.8 | 56.8 | 59.2 | 61.4 | 58.0 | 56.4 | 29.4 | 28.9 | 27.1 |
| 26.0 | 36.4 | 37.0 | 50.0 | 51.0 | 54.6 | 56.7 | 59.9 | 62.7 | 65.3 | 31.4 | 31.7 | 30.3 | 30.0 | 28.2 |
| 26.5 | 36.9 | 37.5 | 51.8 | 53.3 | 57.2 | 59.7 | 63.3 | 66.2 | 69.3 | 32.3 | 32.7 | 31.3 | 30.9 | 29.3 |
| 27.0 | 37.4 | 37.9 | 53.8 | 55.7 | 60.0 | 62.8 | 67.0 | 70.2 | 73.4 | 33.3 | 33.9 | 32.5 | 32.1 | 30.5 |
| 27.5 | 37.8 | 38.3 | 37.8 | 58.4 | 62.6 | 66.1 | 71.0 | 74.4 | 38.6 | 34.6 | 35.3 | 33.9 | 33.4 | 31.9 |
| 28.0 | 38.2 | 38.7 | 38.0 | 61.2 | 65.8 | 69.6 | 75.2 | 49.2 | 38.7 | 36.1 | 36.7 | 35.5 | 34.8 | 33.4 |
| 28.5 | 38.7 | 39.2 | 38.3 | 38.8 | 71.5 | 74.5 | 84.3 | 40.0 | 39.6 | 37.8 | 38.2 | 37.2 | 36.5 | 35.1 |
| 29.0 | 39.1 | 39.7 | 38.8 | 39.1 | 45.2 | 51.8 | 46.6 | 43.8 | 41.1 | (39.4) | 39.8 | (38.9) | 38.2 | 37.0 |
| 29.5 | 39.4 | 40.2 | 39.2 | 39.6 | 44.0 | 46.6 | 45.4 | 46.4 | 43.6 | (41.4) | 41.7 | (41.0) | 40.2 | 39.4 |
| 30.0 | 39.9 | 40.9 | 39.8 | 40.2 | 44.1 | 46.4 | 46.3 | 49.8 | 46.6 | (43.4) | (43.7) | (43.1) | 42.3 | 42.3 |
| 30.5 | 40.4 | 41.6 | 40.5 | 40.9 | 45.1 | 47.4 | 47.7 | (53.8) | 50.5 | (45.4) | (45.6) | (45.6) | 44.7 | (45.9) |
| 31.0 | 40.8 | | | | | | | | | | | | | |

* The brackets indicate extrapolated values.

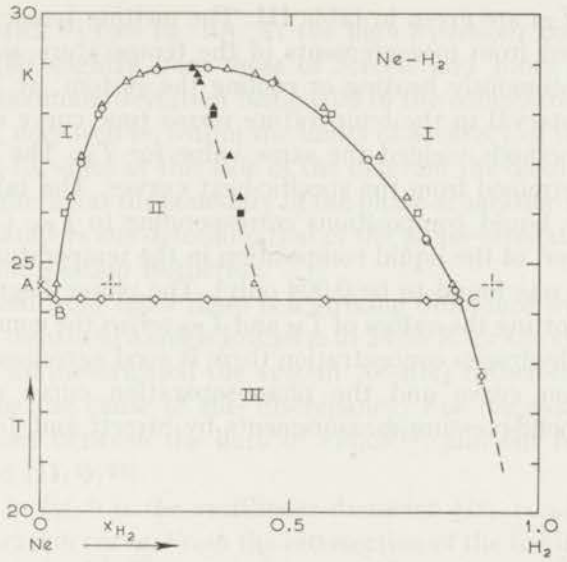


Fig. 9. The phase diagram at vapour–liquid equilibrium pressures for the system Ne–$H_2$.

○ phase-separation temperatures from the present experiment;
◇ melting temperatures from the present experiment;
△ Streett and Jones[12]), ▲ $\frac{1}{2}(x_l + x_u)$;
□ Heck and Barrick[13]), ■ $\frac{1}{2}(x_l + x_u)$;
⊹ Simon[10]);
× triple point Ne[15]);
---- $\frac{1}{2}(x_l + x_u)$ calculated from the separation curve according to the present experiment.

TABLE III

| Transition temperatures | | | | | |
|---|---|---|---|---|---|
| $x_{H_2}$ | $T_M$(K) | $T_{PS}$(K) | $x_{H_2}$ | $T_M$(K) | $T_{PS}$(K) |
| 0.030 | 24.26 | | 0.654 | | 27.08 |
| 0.080 | 24.29 | 27.00 | 0.774 | 24.25 | 25.48 |
| 0.123 | 24.27 | 28.10 | 0.775 | | 25.46 |
| 0.230 | 24.26 | 28.88 | 0.830 | 24.26 | 24.46 |
| 0.334 | 24.27 | 28.83 | 0.840 | 24.27 | |
| 0.463 | | 28.64 | 0.885 | 22.75 | |
| 0.570 | 24.25 | 27.89 | | | |

temperatures and determines the boundary between the phase-separation region II and the homogeneous region I. Below the phase-separation temperature $T_{PS}$ there is an additional contribution to the specific heat due to the heat of mixing, which disappears when the liquid becomes homogeneous.

The results for the melting temperatures $T_M$ and the phase-separation

temperatures $T_{PS}$ are given in table III. The melting temperature $T_M$ has been determined from measurements of the temperature as a function of time while continuously heating or cooling the system; at $T_M$ a constant temperature interval in the temperature *versus* time curve occurs. Within 0.03 K both methods yielded the same value for $T_M$. The values for $T_{PS}$ have been determined from the specific-heat curves. The tabulated values of $x_{H_2}$ are the liquid compositions corresponding to $T_{PS}$. (The maximum change, however, of the liquid composition in the temperature range of the measurements was found to be 0.004 only). The phase diagram in fig. 9 is obtained by plotting the values of $T_M$ and $T_{PS}$ *versus* the composition of the liquid. At low hydrogen concentration there is good agreement between our phase-separation curve and the phase-separation curve obtained from isothermal vapour-pressure measurements by Streett and Jones[12]) and by

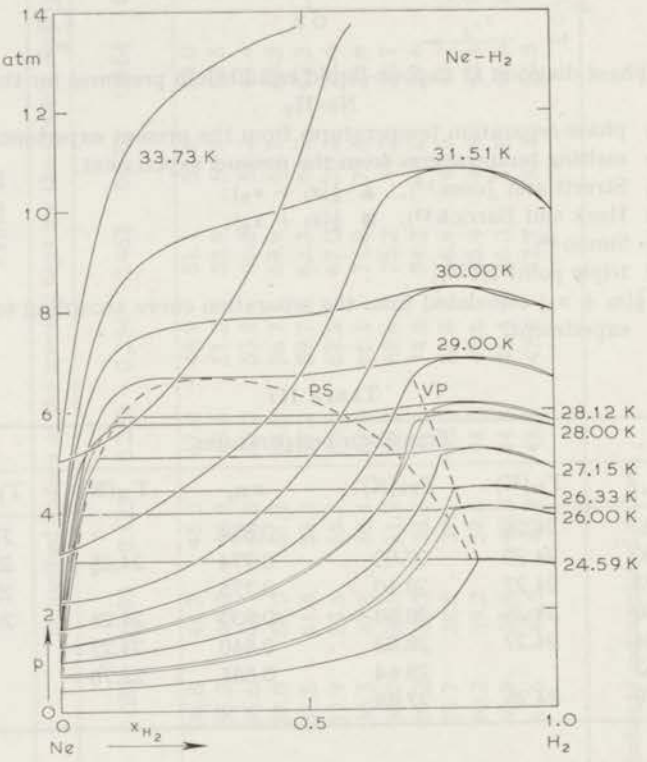


Fig. 10. Pressure-composition diagram for the system Ne–$H_2$.
Isotherms at 24.59 K, 26.33 K, 27.15 K, 28.12 K, 29.00 K, 31.51 K and 33.73 K according to ref. 12.
Isotherms at 26.00 K, 28.00 K and 30.00 K according to ref. 13.
– – – – – PS phase-separation curve;
– – – – – VP pressure-composition curve for the vapour phase in equilibrium with the separated liquid.

Heck and Barrick[13]) (see fig. 10). At the high hydrogen composition side our results differ slightly from those of Streett and Jones and Heck and Barrick, the maximum deviation being 0.03 in the composition. This difference, however, may well be within the limits of accuracy of the experiments of refs. 12 and 13, since at this side of the diagram the discontinuity in the slope of the isotherms at the boundary of the phase-separation region is rather small, which hampers the determination of the phase-separation curve from the pressure-composition isotherms.

As can be seen from fig. 9 there is a striking difference with the data of Simon[10]), who measured a single isotherm at 24.56 K for the system Ne–p$H_2$. The fact that we investigated the system Ne–n$H_2$ rather than Ne–p$H_2$ is not likely to be the cause of this discrepancy. For the system Ne–n$D_2$ a similar difference between the data of Simon[10]) and our results is found (chapters I and III)[11])[24]).

Also shown in fig. 9 is the rectilinear diameter $\frac{1}{2}(x_l + x_u)$ derived from our phase-separation curve. From the intersection of the rectilinear diameter with the phase-separation curve the critical composition of the upper critical consolute point has been obtained. In table IV the experimental results for the critical temperature and critical composition are given.

TABLE IV

The critical consolute point for the system Ne–n$H_2$

| | This experiment | Streett[12]) |
|---|---|---|
| $T_c$ | 28.93 ± 0.03 K | 28.96 ± 0.04 K |
| $x_c$ | 0.308 ± 0.002 | 0.30 |
| $p_c$ | | 6.6[5] atm |

A few corrections to the specific-heat data have still to be mentioned. In the neighbourhood of the transition temperatures $T_M$ and $T_{PS}$ the change of the specific heat with the temperature is quite large, therefore it was necessary to apply the curvature correction[25]) to the specific-heat measurements in these temperature regions.

Due to the difference in composition between vapour and liquid, the composition of the liquid changes as a function of temperature. Since the maximum change is never more than 0.004 over the whole temperature range, the influence of this effect on the specific-heat curves is less than 0.2 J/mole K, and has therefore been neglected.

An idea of the non-systematic errors can be obtained from a plot of the specific heat in the phase-separation region *versus* the liquid composition for different temperatures. According to the leverage rule the specific heat

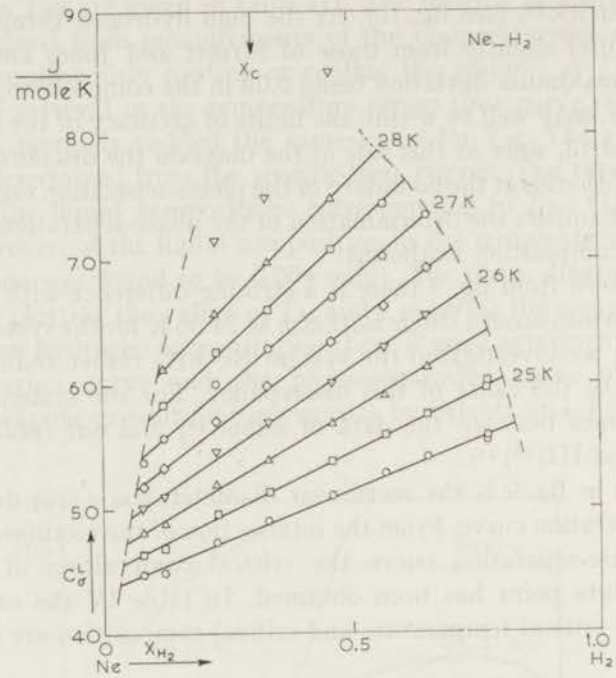


Fig. 11. Specific heat at saturation in the phase-separation region for the system Ne–$H_2$.

in the separation region is given by:

$$c^{\mathrm{L}}_{\bar{x}} = \frac{\bar{x} - x_l}{x_u - x_l} c^{\mathrm{L}}_{x_u} + \frac{x_u - \bar{x}}{x_u - x_l} c^{\mathrm{L}}_{x_l} \qquad (1)$$

and therefore at constant temperature $c^{\mathrm{L}}_{\bar{x}}$ is a linear function of composition. This consistency check has been shown in fig. 11. Below 28 K the deviations from the linear relationship remain within the limits of 2%. Due to the anomalous behaviour of the specific heat near the critical consolute point the data above 28 K are not accurate enough to complete the diagram.

5. *The excess functions**. The thermodynamic excess functions are usually defined as the difference between the thermodynamic functions for the actual system and the values for an ideal mixture at the same pressure, temperature and composition. This definition implies, *e.g.*:

$$\mathscr{H}^{\mathrm{E}}(x, p, T) = H^{\mathrm{M}}(x, p, T) - x\mathrm{H}^0_1(p, T) - (1 - x)\, H^0_2(p, T). \qquad (2)$$

* In the following section the superscript L has been omitted since all quantities refer to the liquid phase.

We may note that the excess enthalpy defined in this way equals the heat of mixing at the pressure $p$ and temperature $T$. If one wants to relate the excess functions for a liquid mixture to the thermodynamic quantities of the pure liquids at their vapour pressures, it is more appropriate to introduce a slightly different definition, *e.g.*:

$$H^{E}(x, p^{M}, T) = H^{M}(x, p^{M}, T) - xH_1^0(p_1^0, T) - (1 - x)\, H_2^0(p_2^0, T), \quad (3)$$

where $p^{M}$ indicates the equilibrium vapour pressure of the mixture and $p_1^0$ and $p_2^0$ the equilibrium vapour pressures of the pure components at the temperature $T$. The excess entropy $S^{E}$ and excess Gibbs function $G^{E}$ are then defined analogously, *e.g.*:

$$S^{E}(x, p^{M}, T) = S^{M}(x, p^{M}, T) - xS_1^0(p_1^0, T) - (1 - x)\, S_2^0(p_2^0, T) + R\{x \ln x + (1 - x) \ln(1 - x)\}. \quad (4)$$

A conversion from these excess functions to the excess functions where the pressure is kept constant at mixing, requires a composition dependent correction in the order of a few percent.

5a. The excess enthalpy. Since mixing occurs when the temperature of the separated liquid mixture is increased, it is possible to derive

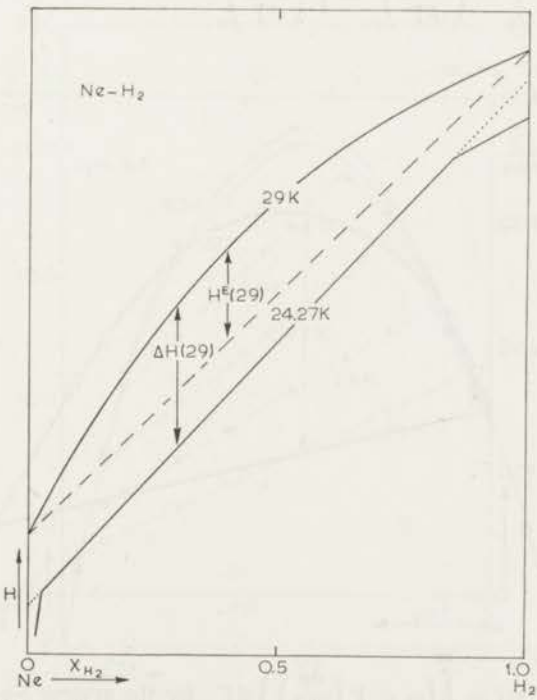


Fig. 12. Schematic enthalpy-composition diagram for the system Ne–$H_2$.

the excess enthalpy by integrating the specific heat of the separated mixture over a temperature interval.

To elucidate the calculation of the excess enthalpy $H^E$ we refer to the schematic enthalpy-composition diagram for the liquid mixture at the liquid-vapour equilibrium pressure in fig. 12. In this diagram the enthalpy-isotherm at 24.27 K (the melting temperature) and at 29 K (just above $T_c$) are shown as a function of composition. The isotherm at 29 K refers to a homogeneous liquid over the whole composition range. At 24.27 K the liquid is separated into two liquid phases with composition $x_l = 0.030$ and $x_u = 0.841$ (see also fig. 9); therefore between these composition limits the enthalpy is a linear function of composition. (The part of the 24.27 K-isotherm for compositions lower than 0.030 represents the enthalpy of the system separated into pure solid neon and a liquid mixture of neon and hydrogen). As can be seen from fig. 12 the enthalpy difference between 24.27 K and 29 K,

$$\Delta H(\bar{x}, 29) = H(\bar{x}, 29) - H(\bar{x}, 24.27),$$

equals $H^E(\bar{x}, 29)$ plus an enthalpy contribution linear in $\bar{x}$, in the composition range $0.030 \leq \bar{x} \leq 0.841$.

Using the identity

$$c_\sigma = T\left(\frac{\partial S}{\partial T}\right)_\sigma = \left(\frac{\partial H}{\partial T}\right)_\sigma - V\left(\frac{\partial p}{\partial T}\right)_\sigma \tag{5}$$

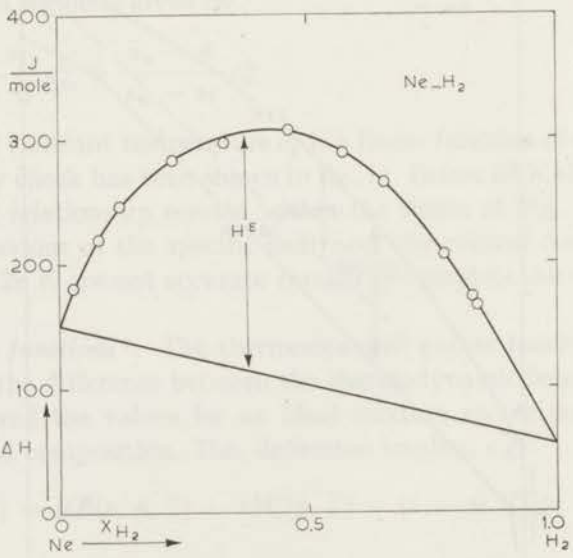


Fig. 13. $\Delta H = \int_{24.27}^{29} \left\{c_\sigma + V\left(\frac{\partial p}{\partial T}\right)_\sigma\right\} dT$ for the system Ne–$H_2$.

we can calculate the enthalpy difference between 24.27 K and 29 K from the measured specific heat:

$$\Delta H(\bar{x}, 29) = \int_{24.27}^{29} \left\{ c_\sigma(\bar{x}, T) + V(\bar{x}, T) \left( \frac{\partial p(\bar{x}, T)}{\partial T} \right)_\sigma \right\} \mathrm{d}T. \tag{6}$$

The second term in the expression for $\Delta H$ accounts for the pressure change and is a correction in the order of 5%.

In fig. 13 the values of $\Delta H(\bar{x}, 29)$ calculated according to eq. (6) have been plotted as a function of $\bar{x}$ for the compositions $0.030 \leq \bar{x} \leq 0.841$. The curve has been extrapolated to $x = 0$ and $x = 1$ and $H^{\mathrm{E}}(\bar{x}, 29)$ is now found from the distance between the curve and the straight line in fig. 13. The part of $\Delta H$ under the straight line is equal to the distance between the two straight lines in fig. 12.

In principle it is possible to calculate in a similar way the excess enthalpy at other temperatures. However, if the upper enthalpy-isotherm in fig. 12 corresponds to a temperature below $T_c$, this isotherm also has a linear part. As a consequence the extrapolation of $\Delta H$ to $x = 0$ and $x = 1$ becomes gradually poorer with decreasing temperatures. Therefore a more accurate way to calculate the excess enthalpy at other temperatures is to use the

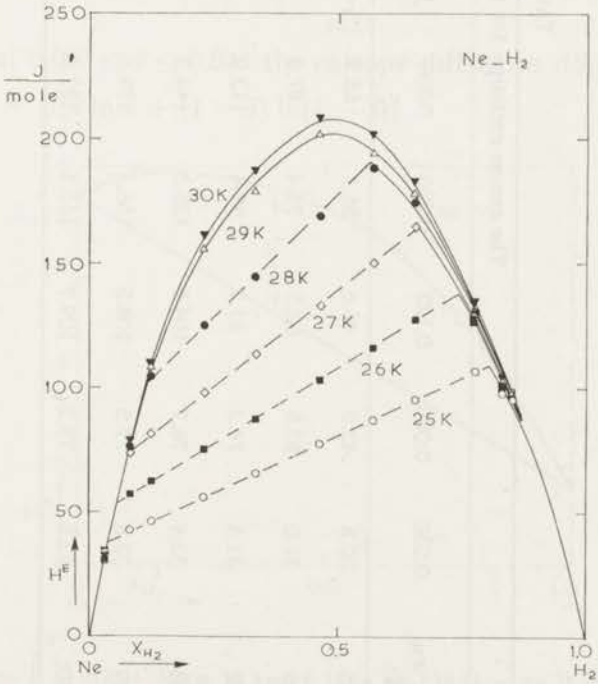


Fig. 14. The excess enthalpy for the system Ne–$H_2$ at different temperatures.

TABLE V

The excess enthalpy for the system Ne–$H_2$ (J/mole)

| $x_{H_2}$ / $T$(K) | 0.030 | 0.080 | 0.123 | 0.230 | 0.334 | 0.463 | 0.570 | 0.654 | 0.774 | 0.775 | 0.830 | 0.840 |
|---|---|---|---|---|---|---|---|---|---|---|---|---|
| 25 | 30.5 | 43.0 | 46.6 | 56.1 | 65.9 | 77.5 | 87.3 | 95.5 | 108.1 | 107.8 | 97.9 | 95.4 |
| 26 | 31.0 | 57.8 | 62.5 | 75.4 | 87.8 | 103.1 | 116.1 | 127.1 | 127.8 | 127.4 | 99.5 | 96.1 |
| 27 | 31.8 | 74.3 | 81.7 | 98.4 | 113.9 | 133.3 | 150.2 | 165.2 | 129.2 | 129.2 | 100.2 | 96.7 |
| 28 | 32.4 | 76.7 | 104.5 | 125.3 | 144.3 | 169.1 | 188.4 | 174.7 | 130.7 | 131.1 | 101.2 | 97.5 |
| 29 | 33.8 | 77.5 | 108.5 | 156.1 | 179.6 | 202.1 | 194.6 | 178.4 | 132.1 | 133.0 | 102.6 | 98.3 |
| 30 | 33.8 | 78.2 | 109.7 | 161.1 | 187.5 | 208.5 | 201.6 | 183.0 | 134.2 | 134.7 | 103.6 | 99.7 |

relation

$$H^{E}(T) = H^{E}(29) + \int_{29}^{T} \left\{ c_{\sigma}^{E}(T) + \left[ V(T) \left( \frac{\partial p(T)}{\partial T} \right)_{\sigma} \right]^{E} \right\} dT. \tag{7}$$

The excess specific heat can be obtained from

$$c_{\sigma}(T) = x c_{\sigma, H_2}^{0}(T) + (1 - x)\, c_{\sigma, Ne}^{0}(T) + c_{\sigma}^{E}(T), \tag{8}$$

and the correction term from

$$\left[ V \left( \frac{\partial p}{\partial T} \right)_{\sigma} \right]^{E} = V \left( \frac{\partial p}{\partial T} \right)_{\sigma} - x V_{H_2}^{0} \left( \frac{dp}{dT} \right)_{H_2}^{0} - (1 - x)\, V_{Ne}^{0} \left( \frac{\partial p}{\partial T} \right)_{Ne}^{0}. \tag{9}$$

In this way the excess enthalpy has been calculated for five other temperatures between 25 K and 30 K. The results are given in fig. 14 and table V.

5b. The excess entropy. For the calculation of the excess entropy $S^{E}$ we follow the same procedure as for the calculation of the excesss enthalpy. The change of entropy between 24.27 K and 29 K along a path of constant composition is obtained from the specific heat using the relation

$$S(\bar{x}, 29) - S(\bar{x}, 24.27) = \Delta S(\bar{x}, 29) = \int_{24.27}^{29} \frac{c_{\sigma}(\bar{x}, T)}{T}\, dT. \tag{10}$$

In the interval $0.030 \leq \bar{x} \leq 0.841$ the entropy difference $\Delta S(\bar{x}, 29)$ equals

$$S^{E}(\bar{x}, 29) - R\{\bar{x} \ln \bar{x} + (1 - \bar{x}) \ln(1 - \bar{x})\}$$

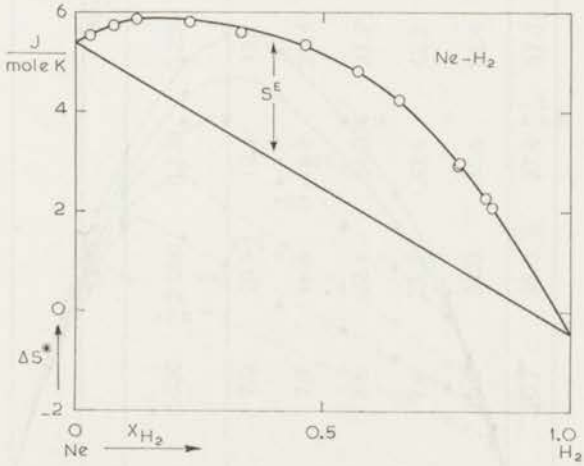


Fig. 15. $\Delta S^{*} = \int_{24.27}^{29} \frac{c_{\sigma}}{T}\, dT + R\{x_{H_2} \ln x_{H_2} + (1 - x_{H_2}) \ln (1 - x_{H_2})\}$ for the system Ne–$H_2$.

plus a linear function in $\bar{x}$. If therefore the quantity

$$\Delta S^*(\bar{x}, 29) = \Delta S(\bar{x}, 29) + R\{\bar{x} \ln \bar{x} + (1 - \bar{x}) \ln(1 - \bar{x})\}$$

is plotted as a function of $\bar{x}$ and the curve is extrapolated to $x = 0$ and $x = 1$ the excess entropy $S^E(\bar{x}, 29)$ is obtained by subtracting the linear contribution from $\Delta S^*$. This graph is represented in fig. 15. From the excess entropy at 29 K, $S^E$ at other temperatures has been calculated using the relation

$$S^E(\bar{x}, T) = S^E(\bar{x}, 29) + \int_{29}^{T} \frac{c_\sigma(\bar{x}, T)}{T} \, dT$$
$$+ S^{\text{id. mixing}}(\bar{x}, 29) - S^{\text{id. mixing}}(\bar{x}, T). \tag{11}$$

The ideal mixing terms on the right-hand side of this equation cancel if the integration path is outside the phase-separation region, but for an integration path from 29 K to a point inside the separation region the difference in ideal entropy of mixing is given by:

$$S^{\text{id. mixing}}(\bar{x}, T) - S^{\text{id. mixing}}(\bar{x}, 29) =$$
$$-R\left[\frac{x_u - \bar{x}}{x_u - x_l}\{x_l \ln x_l + (1 - x_l) \ln(1 - x_l)\}\right.$$
$$\left. + \frac{\bar{x} - x_l}{x_u - x_l}\{x_u \ln x_u + (1 - x_u) \ln(1 - x_u)\}\right]$$
$$+ R\{\bar{x} \ln \bar{x} + (1 - \bar{x}) \ln(1 - \bar{x})\}, \tag{12}$$

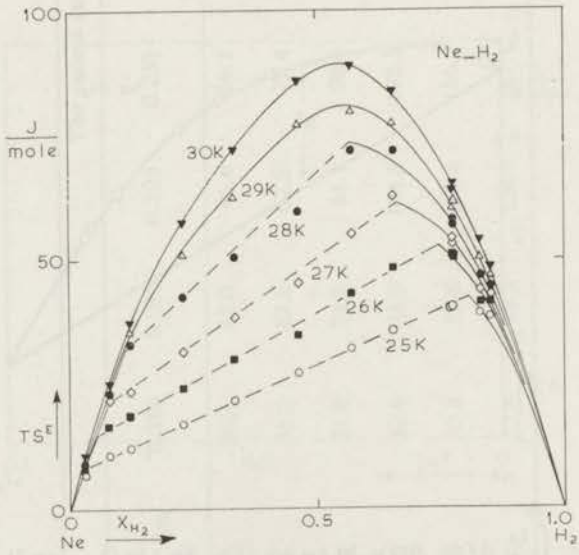


Fig. 16. $TS^E$ for the system Ne–$H_2$ at different temperatures.

TABLE VI

$TS^E$ for the system Ne–$H_2$ (J/mole)

| $T(K)$ \ $x_{H_2}$ | 0.030 | 0.080 | 0.123 | 0.230 | 0.334 | 0.463 | 0.570 | 0.654 | 0.774 | 0.775 | 0.830 | 0.840 |
|---|---|---|---|---|---|---|---|---|---|---|---|---|
| 25 | 7.0 | 10.9 | 12.4 | 17.1 | 21.8 | 27.3 | 32.1 | 35.7 | 40.2 | 40.3 | 39.3 | 38.5 |
| 26 | 7.8 | 16.6 | 18.8 | 24.4 | 30.1 | 35.0 | 43.1 | 48.2 | 50.9 | 50.7 | 41.5 | 41.5 |
| 27 | 8.6 | 22.4 | 24.0 | 31.7 | 38.7 | 45.5 | 55.2 | 62.7 | 53.9 | 54.2 | 44.0 | 42.9 |
| 28 | 9.4 | 23.2 | 33.4 | 42.7 | 50.8 | 59.9 | 72.0 | 71.7 | 56.9 | 57.8 | 46.9 | 44.4 |
| 29 | 10.0 | 24.0 | 35.6 | 51.4 | 62.6 | 77.4 | 79.8 | 77.2 | 60.1 | 61.4 | 50.1 | 46.3 |
| 30 | 10.7 | 25.0 | 37.4 | 57.3 | 71.9 | 85.8 | 89.0 | 83.7 | 63.9 | 65.2 | 53.7 | 48.3 |

where $x_l$ and $x_u$ are the compositions of the two liquids into which the mixture with average composition $\bar{x}$ is separated at temperature $T$.

The results for $TS^E$ are given in table VI and fig. 16.

It may be noted that the accuracy of the calculated excess entropy is seriously influenced by the fact that the contribution from the ideal mixing in $\Delta S$ is of the same order of magnitude as the non-ideal part. Therefore a small inaccuracy in the composition determination of the mixtures, especially near the ends of the composition interval can have a large influence on the extrapolation to $x = 0$ and $x = 1$.

5c. The excess Gibbs function. Using the calculated values for the excess enthalpy and entropy, the excess Gibbs function $G^E$ can be determined from the relation $G^E = H^E - TS^E$. The results for $G^E$ are given in table VII and fig. 17.

From the boiling- and dew-curve measurements of Streett and Jones[12]) it is also possible to calculate the excess chemical potentials using the relation[26])

$$\mu_i^E = RT(x_i^G p^M / x_i^L p_i^0) + (B_{ii} - V_i^L)(p^M - p_i^0), \qquad i = 1, 2. \qquad (13)$$

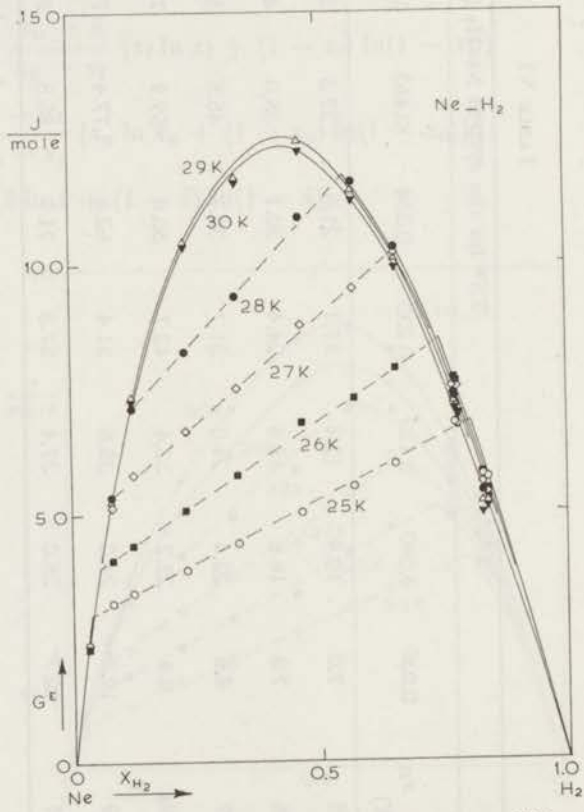


Fig. 17. The excess Gibbs function for the system Ne–$H_2$ at different temperatures.

TABLE VII

The excess Gibbs function for the system Ne–$H_2$ (J/mole)

| $T$(K) \ $x_{H_2}$ | 0.030 | 0.080 | 0.123 | 0.230 | 0.334 | 0.463 | 0.570 | 0.654 | 0.774 | 0.775 | 0.830 | 0.840 |
|---|---|---|---|---|---|---|---|---|---|---|---|---|
| 25 | 23.4 | 32.1 | 34.2 | 39.0 | 44.1 | 50.2 | 55.2 | 59.8 | 67.9 | 67.5 | 57.9 | 56.9 |
| 26 | 23.1 | 41.0 | 43.7 | 50.9 | 57.7 | 68.1 | 73.0 | 78.9 | 76.9 | 76.7 | 58.0 | 54.6 |
| 27 | 23.2 | 51.9 | 57.8 | 66.6 | 75.2 | 87.8 | 95.0 | 102.5 | 75.3 | 75.0 | 56.2 | 53.8 |
| 28 | 23.1 | 53.5 | 71.2 | 82.7 | 93.6 | 109.3 | 116.3 | 103.0 | 73.8 | 73.3 | 54.3 | 53.1 |
| 29 | 23.1 | 53.5 | 73.0 | 104.7 | 117.0 | 124.7 | 114.7 | 101.2 | 72.0 | 71.5 | 52.4 | 52.0 |
| 30 | 23.1 | 53.2 | 72.4 | 103.8 | 116.4 | 122.7 | 112.7 | 99.4 | 70.3 | 69.5 | 50.0 | 51.4 |

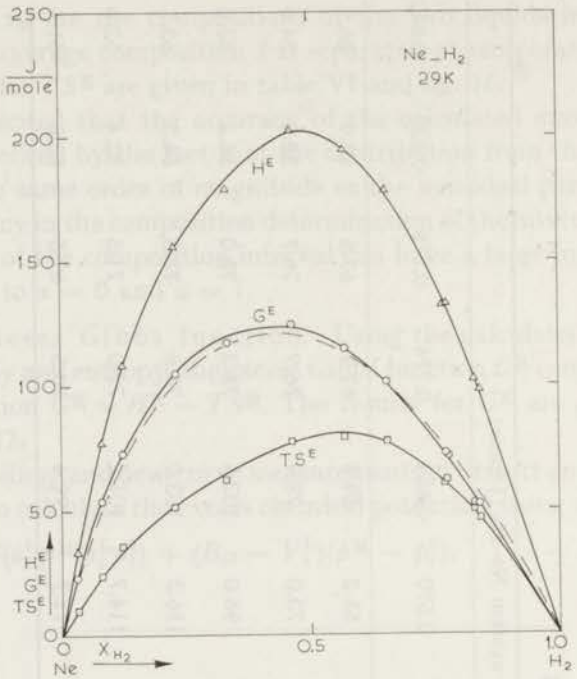


Fig. 18. The excess functions $H^E$, $TS^E$ and $G^E$ at 29 K.
□ $TS^E$; ○ $G^E$; △ $H^E$; ---- $G^E$ calculated from the data of Streett and Jones[12]).

In deriving this equation it is assumed that for the second virial coefficient the relation $2B_{12} = B_{11} + B_{22}$ holds, which implies that the volume excess in the gas phase has been neglected.

We calculated the excess Gibbs function at 29 K with

$$G^E = x^L \mu^E_{H_2} + (1 - x^L)\, \mu^E_{Ne}. \tag{14}$$

The result is shown in fig. 18 together with our results for $G^E$, $H^E$ and $TS^E$ at 29 K. As can be seen from the figure there is a rather good agreement between $G^E$ calculated from the pressure-composition data of Streett and Jones and the $G^E$ obtained from the present experiments. From the values of $G^E$ at different temperatures as calculated from the data of Streett and Jones, $S^E$ can in principle be obtained using the relation

$$S^E = -\left(\frac{\partial G^E}{\partial T}\right)_\sigma + V^E \left(\frac{\partial p}{\partial T}\right)_\sigma. \tag{15}$$

However, for the system Ne–$H_2$ the second term can presumably not be neglected in comparison to $S^E$. Since $V^E$ is not accurately known, no reliable values for $S^E$ can be obtained in this way.

## APPENDIX

*The heat capacity of a two component liquid-vapour system.* Because the expression for the heat capacity of such a system is rather complicated we shall derive the formula by a gradual approach to the actual experimental conditions. First we derive the expression for the heat capacity of a liquid–vapour system in a closed calorimeter assuming a homogeneous liquid phase; in the next step we consider the corrections due to the finite volume of the filling tube of the calorimeter and finally we mention the complications due to the phase separation in the liquid.

Consider a closed calorimeter containing a liquid mixture and some vapour in equilibrium with the liquid and all of the material at a temperature $T$. Such a system has a definite heat capacity since the equilibrium state of the thermodynamic system is completely defined by the temperature alone. The heat capacity of the content of the calorimeter can therefore be derived from the total entropy $\mathcal{S}^{\mathrm{tot}}$ of the system:

$$C = T\frac{\mathrm{d}\mathcal{S}^{\mathrm{tot}}}{\mathrm{d}T} = T\frac{\mathrm{d}}{\mathrm{d}T}(N^{\mathrm{L}}S^{\mathrm{L}} + N^{\mathrm{G}}S^{\mathrm{G}}). \tag{A.1}$$

Since the system is closed the molar balance is expressed by the following relations:

$$N^{\mathrm{L}} + N^{\mathrm{G}} = N^{\mathrm{tot}} = \text{constant}, \tag{A.2}$$

$$N^{\mathrm{L}}x^{\mathrm{L}} + N^{\mathrm{G}}x^{\mathrm{G}} = N^{\mathrm{tot}}\langle x\rangle = \text{constant}. \tag{A.3}$$

For a fixed charge of the calorimeter the quantities $N^{\mathrm{L}}$, $N^{\mathrm{G}}$, $x^{\mathrm{L}}$, $x^{\mathrm{G}}$ and the pressure $p$ will be definite functions of the temperature $T$. These functions can be calculated if the molar volumes of the liquid and vapour and the equilibrium pressure-composition data are known. Assuming that $N^{\mathrm{L}}(T)$, $N^{\mathrm{G}}(T)$, $x^{\mathrm{L}}(T)$, $x^{\mathrm{G}}(T)$ and $p(T)$ can be calculated, we write for one mole of liquid:

$$T\frac{\mathrm{d}S^{\mathrm{L}}}{\mathrm{d}T} = T\left(\frac{\partial S^{\mathrm{L}}}{\partial T}\right)_{x^{\mathrm{L}},p} + T\left(\frac{\partial S^{\mathrm{L}}}{\partial p}\right)_{x^{\mathrm{L}},T}\frac{\mathrm{d}p}{\mathrm{d}T} + T\left(\frac{\partial S^{\mathrm{L}}}{\partial x^{\mathrm{L}}}\right)_{p,T}\frac{\mathrm{d}x^{\mathrm{L}}}{\mathrm{d}T}, \tag{A.4}$$

and for one mole of gas:

$$T\frac{\mathrm{d}S^{\mathrm{G}}}{\mathrm{d}T} = T\left(\frac{\partial S^{\mathrm{G}}}{\partial T}\right)_{x^{\mathrm{G}},p} + T\left(\frac{\partial S^{\mathrm{G}}}{\partial p}\right)_{x^{\mathrm{G}},T}\frac{\mathrm{d}p}{\mathrm{d}T} + T\left(\frac{\partial S^{\mathrm{G}}}{\partial x^{\mathrm{G}}}\right)_{p,T}\frac{\mathrm{d}x^{\mathrm{G}}}{\mathrm{d}T}. \tag{A.5}$$

The molar entropies of the liquid and vapour are related to the molar entropies of the pure components at the pressure $p$ and temperature $T$ of

the mixture by the equations

$$S^{L}(x^{L}, p, T) = x^{L}S_1^{0L}(p, T) + (1 - x^{L})\, S_2^{0L}(p, T) + \mathscr{S}^{\text{mixing, L}}(x^{L}, p, T), \tag{A.6}$$

$$S^{G}(x^{G}, p, T) = x^{G}S_1^{0G}(p, T) + (1 - x^{G})\, S_2^{0G}(p, T) + \mathscr{S}^{\text{mixing, G}}(x^{G}, p, T). \tag{A.7}$$

The molar entropies of mixing are given by:

$$\mathscr{S}^{\text{mixing, L}}(x^{L}, p, T) = -R\{x^{L}\ln x^{L} + (1-x^{L})\ln(1-x^{L})\} + \mathscr{S}^{\text{E, L}}(x^{L}, p, T), \tag{A.8}$$

$$\mathscr{S}^{\text{mixing, G}}(x^{G}, p, T) = -R\{x^{G}\ln x^{G} + (1-x^{G})\ln(1-x^{G})\} + \mathscr{S}^{\text{E, G}}(x^{G}, p, T), \tag{A.9}$$

where the excess molar entropies $\mathscr{S}^{\text{E, L}}$ and $\mathscr{S}^{\text{E, G}}$ are thus defined as the difference between the molar entropy of a real mixture and the molar entropy of an ideal mixture at the same pressure $p$ and temperature $T$.

For the total heat capacity $C$ of the content of the calorimeter we now obtain, by rewriting eq. (A.1) using eqs. (A.3)–(A.9),

$$\begin{aligned} C = {} & T\left\{\left(\frac{\partial S^{L}}{\partial T}\right)_{x^{L}, p} + \left(\frac{\partial S^{L}}{\partial p}\right)_{x^{L}, T}\frac{\mathrm{d}p}{\mathrm{d}T}\right\} N^{L} \\ & + T\left\{\left(\frac{\partial S^{G}}{\partial T}\right)_{x^{G}, p} + \left(\frac{\partial S^{G}}{\partial p}\right)_{x^{G}, T}\frac{\mathrm{d}p}{\mathrm{d}T}\right\} N^{G} \\ & - T(S_1^{0G} - S_1^{0L})\,\frac{\mathrm{d}N^{L}x^{L}}{\mathrm{d}T} - T(S_2^{0G} - S_2^{0L})\,\frac{\mathrm{d}N^{L}(1 - x^{L})}{\mathrm{d}T} \\ & + T(\mathscr{S}^{\text{mixing, L}} - \mathscr{S}^{\text{mixing, G}})\,\frac{\mathrm{d}N^{L}}{\mathrm{d}T} \\ & + T\left(\frac{\partial \mathscr{S}^{\text{mixing, L}}}{\partial x^{L}}\right)_{p, T}\frac{\mathrm{d}x^{L}}{\mathrm{d}T}\, N^{L} + T\left(\frac{\partial \mathscr{S}^{\text{mixing, G}}}{\partial x^{G}}\right)_{p, T}\frac{\mathrm{d}x^{G}}{\mathrm{d}T}\, N^{G}. \end{aligned} \tag{A.10}$$

The first term in this expression is the leading term when the content of the calorimeter is predominantly in the liquid phase. This term can immediately be related to the specific heat of the liquid along the saturation line at constant composition, $c_{\sigma}^{L}$ by the following equation:

$$\begin{aligned} & T\left\{\left(\frac{\partial S^{L}}{\partial T}\right)_{x^{L}, p} + \left(\frac{\partial S^{L}}{\partial p}\right)_{x^{L}, T}\frac{\mathrm{d}p}{\mathrm{d}T}\right\} \\ & \quad = T\left\{\left(\frac{\partial S^{L}}{\partial T}\right)_{x^{L}, p} + \left(\frac{\partial S^{L}}{\partial p}\right)_{x^{L}, T}\left(\frac{\partial p}{\partial T}\right)_{x^{L}} + \left(\frac{\partial S^{L}}{\partial p}\right)_{x^{L}, T}\left(\frac{\partial p}{\partial x^{L}}\right)_{T}\frac{\mathrm{d}x^{L}}{\mathrm{d}T}\right\} \\ & \quad = c_{\sigma}^{L} - T\left(\frac{\partial V^{L}}{\partial T}\right)_{x^{L}, p}\left(\frac{\partial p}{\partial x^{L}}\right)_{T}\frac{\mathrm{d}x^{L}}{\mathrm{d}T}. \end{aligned} \tag{A.11}$$

For the second term of eq. (A.10) we find

$$T\left\{\left(\frac{\partial S^{\mathrm{G}}}{\partial T}\right)_{x^{\mathrm{G}},p}+\left(\frac{\partial S^{\mathrm{G}}}{\partial p}\right)_{x^{\mathrm{G}},T}\frac{\mathrm{d}p}{\mathrm{d}T}\right\}=c^{\mathrm{G}}_{p,x^{\mathrm{G}}}-T\left(\frac{\partial V^{\mathrm{G}}}{\partial T}\right)_{x^{\mathrm{G}},p}\frac{\mathrm{d}p}{\mathrm{d}T}. \quad \text{(A.12)}$$

Since in the term $T(S_1^{0\mathrm{G}}-S_1^{0\mathrm{L}})$ of eq. (A.10) $S_1^{0\mathrm{G}}$ and $S_1^{0\mathrm{L}}$ are to be taken at pressure $p$ and temperature $T$ of the mixture, they may refer to a fictitious physical situation. Therefore we shall relate $T(S_1^{0\mathrm{G}}-S_1^{0\mathrm{L}})$ to the heat of evaporation of the pure substance at temperature $T$ and at the corresponding equilibrium vapour pressure $p_1^0$ for the pure species 1:

$$\begin{aligned}T\{S_1^{0\mathrm{G}}(p,T)-S_1^{0\mathrm{L}}(p,T)\}&=T\{S_1^{0\mathrm{G}}(p_1^0,T)-S_1^{0\mathrm{L}}(p_1^0,T)\}\\&+T\int_{p_1^0}^{p}\left\{\left(\frac{\partial S_1^{0\mathrm{G}}(p,T)}{\partial p}\right)_T-\left(\frac{\partial S_1^{0\mathrm{L}}(p,T)}{\partial p}\right)_T\right\}\mathrm{d}p\\&=\Delta_{\mathrm{e}}H_1^0(p_1^0,T)-T\int_{p_1^0}^{p}\left\{\left(\frac{\partial V_1^{0\mathrm{G}}}{\partial T}\right)_p-\left(\frac{\partial V_1^{0\mathrm{L}}}{\partial T}\right)_p\right\}\mathrm{d}p\\&=\Delta_{\mathrm{e}}H_1^0(p_1^0,T)-RT\ln\frac{p}{p_1^0},\end{aligned} \quad \text{(A.13)}$$

where $\Delta_{\mathrm{e}}H_1^0(p_1^0,T)$ denotes the heat of evaporation of the pure substance at temperature $T$. For the second term on the right-hand side in eq. (A.13) the gas phase has been taken ideal and the contribution from $(\partial V_1^{0\mathrm{L}}/\partial T)_p$ has been neglected. In a similar way $T(S_2^{0\mathrm{G}}-S_2^{0\mathrm{L}})$ can be related to the heat of evaporation of species 2 at its equilibrium pressure $p_2^0$. Rewriting the first three terms in eq. (A.10) using eqs. (A.11), (A.12) and (A.13) we find:

$$\begin{aligned}C&=N^{\mathrm{L}}c_\sigma^{\mathrm{L}}-N^{\mathrm{L}}T\left(\frac{\partial V^{\mathrm{L}}}{\partial T}\right)_{x^{\mathrm{L}},p}\left(\frac{\partial p}{\partial x^{\mathrm{L}}}\right)_T\frac{\mathrm{d}x^{\mathrm{L}}}{\mathrm{d}T}\\&+N^{\mathrm{G}}\left\{c_p^{\mathrm{G}}-T\left(\frac{\partial V^{\mathrm{G}}}{\partial T}\right)_{x^{\mathrm{G}},p}\frac{\mathrm{d}p}{\mathrm{d}T}\right\}\\&-\left(\Delta_{\mathrm{e}}H_1^0-RT\ln\frac{p}{p_1^0}\right)\frac{\mathrm{d}N^{\mathrm{L}}x^{\mathrm{L}}}{\mathrm{d}T}\\&-\left(\Delta_{\mathrm{e}}H_2^0-RT\ln\frac{p}{p_2^0}\right)\frac{\mathrm{d}N^{\mathrm{L}}(1-x^{\mathrm{L}})}{\mathrm{d}T}\\&+T\left(\mathscr{S}^{\mathrm{mixing,L}}-\mathscr{S}^{\mathrm{mixing,G}}\right)\frac{\mathrm{d}N^{\mathrm{L}}}{\mathrm{d}T}\\&+TN^{\mathrm{L}}\left(\frac{\partial\mathscr{S}^{\mathrm{mixing,L}}}{\partial x^{\mathrm{L}}}\right)_{p,T}\frac{\mathrm{d}x^{\mathrm{L}}}{\mathrm{d}T}\\&+TN^{\mathrm{G}}\left(\frac{\partial\mathscr{S}^{\mathrm{mixing,G}}}{\partial x^{\mathrm{G}}}\right)_{p,T}\frac{\mathrm{d}x^{\mathrm{G}}}{\mathrm{d}T}.\end{aligned} \quad \text{(A.14)}$$

In this expression the first term on the right hand side is the heat capacity of the liquid, while the other terms constitute the vapour correction.

Up to now we considered a closed calorimeter. If the calorimeter has a filling tube which contains a part of the vapour phase, pressure, temperature and composition of the vapour in the filling tube change during the experiment.

For the calculation of the molar balance it is important to realize that the liquid as well as the vapour are frequently stirred during the experiment. We may therefore assume that the composition of the vapour in the filling tube is always equal to the composition of the vapour in the calorimeter, *i.e.* $x_c^G = x_t^G$. Under this condition, knowing also the temperature gradient along the filling tube, the molar distribution in the apparatus can again be calculated as a function of the temperature of the calorimeter. The molar balance is now expressed by the equations

$$N^L + N^G + N_t^G = N^{tot} = \text{constant}, \tag{A.15}$$

$$N^L x^L + N^G x^G + N_t^G x^G = N^{tot} \langle x \rangle = \text{constant}. \tag{A.16}$$

For the vapour correction the main difference compared to the closed calorimeter is that now vapour expands in the filling tube when the temperature increases, causing therefore a larger evaporation. To account for the larger evaporation we consider the process in the apparatus during a single heating period. The actual change of the system in this process may be realized in two steps. For the first step a weightless piston is thought to be present at the lower end of the filling tube, which is allowed to move in the tube during the heating in order to establish pressure equilibrium. In the second step the piston is again removed so that the vapour in the tube obtains the equilibrium composition. If the actual process is approximated with the hypothetical process in the first step only, the composition change in the filling tube during the real process is neglected. It can, however, be shown that such an approximation is justified when the molar content of the filling tube is small compared to the molar content of the calorimeter. The change of composition in the tube then has a negligible influence on the composition of the liquid and as a consequence the pressure change in the system, which is a function of temperature and liquid composition, is nearly independent of the composition change in the tube.

The heat capacity of the calorimeter content for the above mentioned hypothetical process can be derived similarly as for the closed calorimeter; only the molar balance equations (A.2) and (A.3) have to be replaced by:

$$N^L + N^G = N' = \text{constant}, \tag{A.17}$$

$$N^L x^L + N^G x^G = N' \langle x \rangle' = \text{constant}, \tag{A.18}$$

where $N'$ is the molar content of the calorimeter and $\langle x \rangle'$ the mean compo-

sition in the calorimeter, as obtained from eqs. (A.15) and (A.16) and where these quantities assume a new value for each temperature.

We may thus conclude that, for a properly charged calorimeter, eq. (A.14) still holds if the temperature derivatives of the quantities $N^{\mathrm{L}}$, $N^{\mathrm{G}}$, $x^{\mathrm{L}}$ and $x^{\mathrm{G}}$ are taken in accordance with eqs. (A.17) and (A.18).

We finally consider the phase separation in the liquid. The molar entropy of the liquid in the two-phase region is given according to the leverage rule by

$$S^{\mathrm{L}} = \frac{\bar{x} - x_l}{x_u - x_l} S_u^{\mathrm{L}} + \frac{x_u - \bar{x}}{x_u - x_l} S_l^{\mathrm{L}}. \tag{A.19}$$

Therefore $\mathscr{S}^{\mathrm{mixing,L}}$ in eq. (A.6) takes a more complicated form than given in eq. (A.8) because of the phase separation:

$$\mathscr{S}^{\mathrm{mixing,L}} = \frac{\bar{x} - x_l}{x_u - x_l} [\mathscr{S}_u^{\mathrm{E,L}} - R\{x_u \ln x_u + (1 - x_u) \ln(1 - x_u)\}]$$

$$+ \frac{x_u - \bar{x}}{x_u - x_l} [\mathscr{S}_l^{\mathrm{E,L}} - R\{x_l \ln x_l + (1 - x_l) \ln(1 - x_l)\}]. \tag{A.20}$$

As a consequence we must use for the entropy of mixing of the liquid in eq. (A.14) the expression as given in eq. (A.20) when the liquid is separated, while we must use eq. (A.8) in the homogeneous region.

## REFERENCES


1) De Bruyn Ouboter, R., Taconis, K. W., Le Pair, C. and Beenakker, J. J. M., Physica **26** (1960) 853.
2) Knaap, H. F. P., Knoester, M. and Beenakker, J. J. M., Physica **27** (1961) 309; Knaap, H. F. P., Van Heijningen, R. J. J., Korving, J. and Beenakker, J. J. M., Physica **28** (1962) 343.
3) Newman, R. B. and Jackson, L. C., Trans. Faraday Soc. **54** (1958) 1481.
4) Lambert, M., Phys. Rev. Letters **4** (1960) 555.
5) De Boer, J., Physica **14** (1948) 139.
6) Prigogine, I., The molecular theory of solutions (North-Holland Publ. Cy., Amsterdam, 1957).
7) Beenakker, J. J. M. and Knaap, H. F. P., Progress in low Temp. Phys., ed. C. J. Gorter (North-Holland Publ. Cy., Amsterdam), Vol. V, chap. 7.
8) Hirschfelder, J. O., Curtiss, C. F. and Bird, R. B., Molecular theory of gases and liquids (John Wiley, New York, 1954).
9) Michels, A., De Graaff, W. and Ten Seldam, C. A., Physica **26** (1960) 393.
10) Simon, M., Physica **29** (1963) 1079; Phys. Letters **2** (1962) 234; Phys. Letters **5** (1963) 319.
11) Brouwer, J. P., Hermans, L. J. F., Knaap, H. F. P. and Beenakker, J. J. M., Physica **30** (1964) 1409.
12) Streett, W. B. and Jones, C. H., J. chem. Phys. **42** (1965) 3989.

13) Heck, C. K. and Barrick, P. L., Advances Cryog. Engng **11** (1966) 349.
14) The International Practical Temperature Scale of 1968, Metrologia **5** (1969) 35.
15) Grilly, E. R., Cryogenics **2** (1962) 226.
16) Bigeleisen, J. and Roth, E., J. chem. Phys. **35** (1961) 68.
17) Woolley, H. W., Scott, R. B. and Brickwedde, F. G., J. Res. Nat. Bur. Stand **41** (1948) 379.
18) Friedman, A. S., Nat. Bur. Stand. Rept. 3282.
19) McCarthy, R. D. and Stewart. R. B., Nat. Bur. Stand., Rept. 8726.
20) Younglove, B. A. and Diller, D. E., Cryogenics **2** (1962) 283.
21) Clusius, K., Z. phys. Chem. **B31** (1936) 459.
22) Fagerstroem, C. H. and Hollis–Hallett, A. C., Proc. intern. Conf. low Temp. Phys., 9th., Columbus, Ohio, 1964 B (1965) 1092.
23) Clusius, K., Flubacher, P., Piesbergen, U., Schleich, K., and Sperandio, A., Z. Naturforsch. **15a** (1960) 1.
24) Brouwer, J. P., Van den Meijdenberg, C. J. N. and Beenakker, J. J. M., Physica (1970), to be published.
25) Osborne, N. S., Steinson, H. F., Sligh, T. S. and Cragoe, C. S., Sci. Papers Nat. Bur. Stand. **20** (1925) 66.
26) Scatchard, G. and Raymond, C. L., J. Amer. Chem. Soc. **60** (1938) 1278.

CHAPTER III

# SPECIFIC HEAT OF THE LIQUID MIXTURES OF NEON AND HYDROGEN ISOTOPES IN THE PHASE-SEPARATION REGION.

## THE SYSTEM Ne–$D_2$

**Synopsis**

The phase separation in the liquid binary system of neon and normal deuterium has been investigated by measuring the specific heat at saturation for different compositions between 24 K and 27.5 K. The phase-separation curve has been determined. The coordinates of the upper critical consolute point are $T_c = 25.71$ K and $x_{D_2} = 0.354$. The temperature at which the two-liquid region is terminated by the solidification of the neon is $T_M = 23.86$ K. The excess enthalpy, the excess entropy and the excess Gibbs function of the liquid mixtures have been calculated as a function of temperature and composition.

For the systems Ne–n$H_2$ and Ne–n$D_2$ the critical coefficient $\beta$ has been determined from the shape of the phase-separation curve. Finally a comparison of the experimental results with the results of Prigogine's theory for isotopic mixtures of quantum fluids has been made. Only qualitative agreement has been found.

1. *Introduction.* As has been indicated in the previous chapter [1]) specific-heat measurements on liquid mixtures of neon and the hydrogen isotopes are appropriate for studying the influence of the zero-point energy on the thermodynamic properties of isotopic mixtures. From the data on the specific heat in the temperature range where the liquid separates into two phases, the excess enthalpy, the excess entropy and the excess Gibbs function can be calculated. In chapter II the measurements and results for the system Ne–$H_2$ have been presented, whereas in this chapter the results for the system Ne–$D_2$ will be presented.

In section 2 an account of the experimental details for the system Ne–$D_2$ is given. In section 3 the calculation of the vapour correction for the present system is discussed. In section 4 the results of the specific-heat measurements

and the phase diagram are presented and in section 5 the calculation of the excess functions is given. In section 6 we consider for both Ne–$D_2$ as well as Ne–$H_2$ the phenomena occurring in the neighbourhood of the critical point, while in section 7 the experimental results for the thermodynamic excess functions of both systems are compared with the theory for isotopic mixtures of Prigogine and his group[2]).

For the notations used in this chapter we refer to the list in chapter II.

2. *Experimental method.* The apparatus and experimental setup used for the experiments on the system Ne–$D_2$ are the same as used for the experiments on the system Ne–$H_2$. For the details on the calorimeter, the calibration of the thermometer and the experimental technique we refer to the work on Ne–$H_2$[1]).

From a mass spectrometer analysis of the deuterium used in these experiments, the isotopic composition was found to be 99.47% $D_2$, 0.37% $H_2$ and 0.16% HD. Although in such an analysis $D_2$ could not be distinguished from He, the presence of He in the samples is very unlikely, since the deuterium was prepared from heavy water by electrolysis. The isotopic composition of the Ne was found to be 90.53% $^{20}$Ne, 0.33% $^{21}$Ne and 9.14% $^{22}$Ne, which is nearly equal to the natural abundance. The amount of He in the neon was smaller than 0.01%. The measurements of the specific heat have been performed with normal deuterium, *i.e.* 66.7% ortho $D_2$ and 33.3% para $D_2$.

3. *Calculation of the vapour correction.* The expression for the total heat capacity of a two component liquid-vapour system has been derived in the appendix of the previous chapter:

$$
\begin{aligned}
C = {} & N^{\mathrm{L}} c_{\sigma}^{\mathrm{L}} - N^{\mathrm{L}} T \left( \frac{\partial V^{\mathrm{L}}}{\partial T} \right)_{x^{\mathrm{L}}, p} \left( \frac{\partial p}{\partial x^{\mathrm{L}}} \right)_{T} \frac{\mathrm{d}x^{\mathrm{L}}}{\mathrm{d}T} \\
& + N^{\mathrm{G}} \left\{ c_{p}^{\mathrm{G}} - T \left( \frac{\partial V^{\mathrm{G}}}{\partial T} \right)_{x^{\mathrm{G}}, p} \frac{\mathrm{d}p}{\mathrm{d}T} \right\} \\
& - \left( \Delta_{\mathrm{e}} H_1^0 - RT \ln \frac{p}{p_1^0} \right) \frac{\mathrm{d}N^{\mathrm{L}} x^{\mathrm{L}}}{\mathrm{d}T} \\
& - \left( \Delta_{\mathrm{e}} H_2^0 - RT \ln \frac{p}{p_2^0} \right) \frac{\mathrm{d}N^{\mathrm{L}} (1 - x^{\mathrm{L}})}{\mathrm{d}T} \\
& + T (\mathscr{S}^{\mathrm{mixing,\,L}} - \mathscr{S}^{\mathrm{mixing,\,G}}) \frac{\mathrm{d}N^{\mathrm{L}}}{\mathrm{d}T} \\
& + T N^{\mathrm{L}} \left( \frac{\partial \mathscr{S}^{\mathrm{mixing,\,L}}}{\partial x^{\mathrm{L}}} \right)_{p, T} \frac{\mathrm{d}x^{\mathrm{L}}}{\mathrm{d}T} + T N^{\mathrm{G}} \left( \frac{\partial \mathscr{S}^{\mathrm{mixing,\,G}}}{\partial x^{\mathrm{G}}} \right)_{p, T} \frac{\mathrm{d}x^{\mathrm{G}}}{\mathrm{d}T}.
\end{aligned}
\qquad \text{(II, A.14)}
$$

This expression, involving a rather complicated vapour correction in the case of Ne–$H_2$, can be simplified considerably for the system Ne–$D_2$. Since for the liquid Ne–$D_2$ mixture in the temperature range between 24 K and 30 K, the thermal expansion is much smaller than for the liquid Ne–$H_2$ mixture, for Ne–$D_2$ it is possible to fill the calorimeter nearly completely with liquid at the lowest temperature of a run. Moreover for this system the change of the vapour pressure is smaller. As a consequence the amount of liquid evaporating during a run is much smaller for the system Ne–$D_2$ than for Ne–$H_2$ and therefore the change of the liquid composition is also smaller. Actually for the system Ne–$D_2$ the change of the liquid composition during a run was found to be approximately 0.0002. Under this condition it can be shown that terms containing $dx^L/dT$ contribute less than 0.2% to the total heat capacity $C$ and may therefore be neglected. Neglecting moreover the excess entropy in the gas phase, eq. (II, A.14) reduces to the form:

$$C = N^L c_\sigma^L + N^G \left( c_p^G - T \left( \frac{\partial V^G}{\partial T} \right)_{x^G, p} \frac{dp}{dT} \right) - \left\{ x^L \Delta_e H_1^0 + (1 - x^L)\, \Delta_e H_2^0 - RT \left( x^L \ln \frac{p}{p_1^0} + (1 - x^L) \ln \frac{p}{p_2^0} \right) - T \mathscr{S}^{\text{mixing, L}} \right\} \frac{dN^L}{dT}. \quad (1)$$

In this expression the first term denotes the heat capacity of the liquid at constant liquid composition along the vapour line, the second term the heat capacity of the vapour and the last term the contribution to the total heat capacity resulting from the evaporation of liquid at the pressure $p$ and the temperature $T$ of the mixture.

From the dimensions of the apparatus, the properties of the pure components[3, 4, 5]) and the liquid-vapour equilibrium data of the system Ne–$D_2$[6]) the distribution of moles between liquid and gas phase was calculated as a function of temperature. Once $N^L(T)$, $N^G(T)$, $x^L(T)$, $x^G(T)$ and $p(T)$ were known, the vapour correction was calculated at 0.5 K intervals between 24 K and 27 K according to eq. (1). The small correction involving $\mathscr{S}^{E,L}$ was finally evaluated by calculating $\mathscr{S}^{E,L}$ from the first approximation of the specific heat (see section 5). As $dN^L/dT$ is considerably smaller for Ne–$D_2$ than for Ne–$H_2$ the total vapour correction never exceeded 2% for the present measurements.

4. *Experimental results.* In fig. 1 the smoothed values for the specific heat of normal $D_2$ and Ne at saturation are given as a function of temperature. The results for Ne have been discussed in chapter II. The data of Kerr *et al.*[7]), who measured the specific heat of liquid ortho $D_2$ in the temperature range from 19 K up to 23 K only, are also presented in fig. 1.

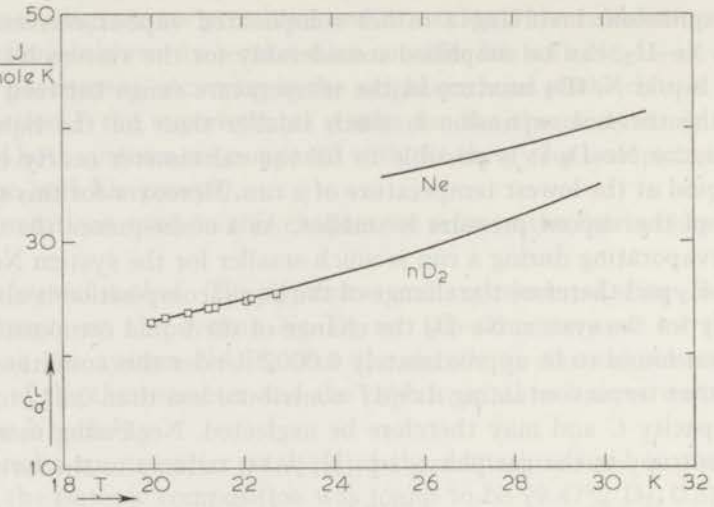


Fig. 1. The specific heat at saturation of $nD_2$ and Ne.
——— smoothed values of the present research;
□ $oD_2$, Kerr *et al.*[7]).

As the rotational contribution to the specific heat of ortho $D_2$ becomes of importance above 25 K only, there is no reason to expect a significant difference in results for the two modifications between 20 K and 23 K.

In fig. 2 a deviation plot for the specific-heat data of deuterium is given. Our specific-heat data appear to be in perfect agreement with those of Kerr *et al.* at 20 K, but are approximately 1% larger at 23 K. The maximal scattering of our points remains within 1%. In chapter II we found for

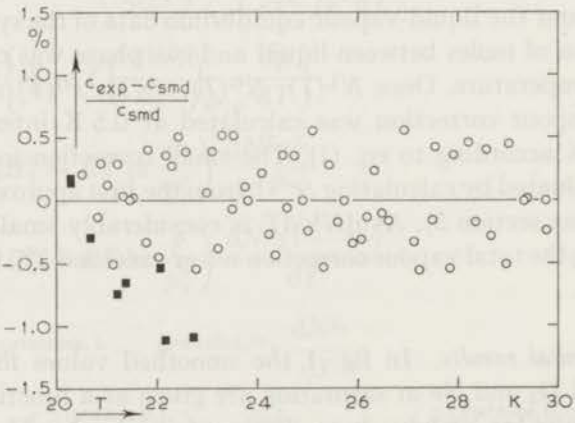


Fig. 2. Deviations of the measured specific heat of $D_2$ from the smoothed values of the present research.
○ $nD_2$, this research; ■ $oD_2$, Kerr *et al.*[7]).

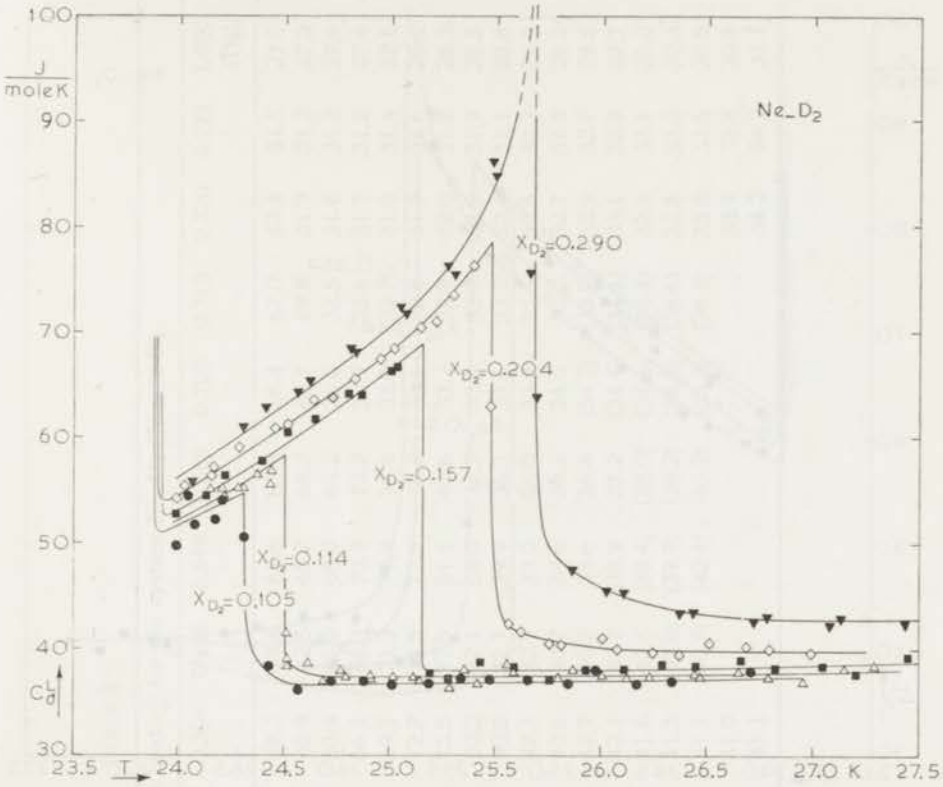


Fig. 3. Specific heat at saturation for the system Ne–$D_2$, for compositions $x_{D_2} < 0.3$.

Ne and $pH_2$ a scattering of 2%. It was found that stirring unfavourably affected the accuracy of the specific-heat measurements. Since for the pure components it was not really necessary to stir, no stirring was applied for the pure $D_2$, resulting in an increased accuracy.

The results of the specific-heat measurements of the liquid mixtures are given in figs. 3, 4 and 5 for 13 different compositions. The specific-heat data have been corrected for the curvature in the neighbourhood of the transition temperatures[8]). The scattering of the points is in the order of 2%, which again is a consequence of the stirring during these measurements. The smoothed specific-heat values at 0.2 K intervals are given in table I, for the compositions at which the measurements were performed.

The phase diagram shown in fig. 6 has been obtained in the following way. The melting temperature $T_M$ (at 23.86 K) has been determined as the temperature at which there is a flat section in the temperature *versus* time curve when the liquid mixture is carefully cooled down or the solidified mixture is carefully heated. The phase-separation temperatures $T_{PS}$ have been determined from the peaks in the specific-heat curves, which occur

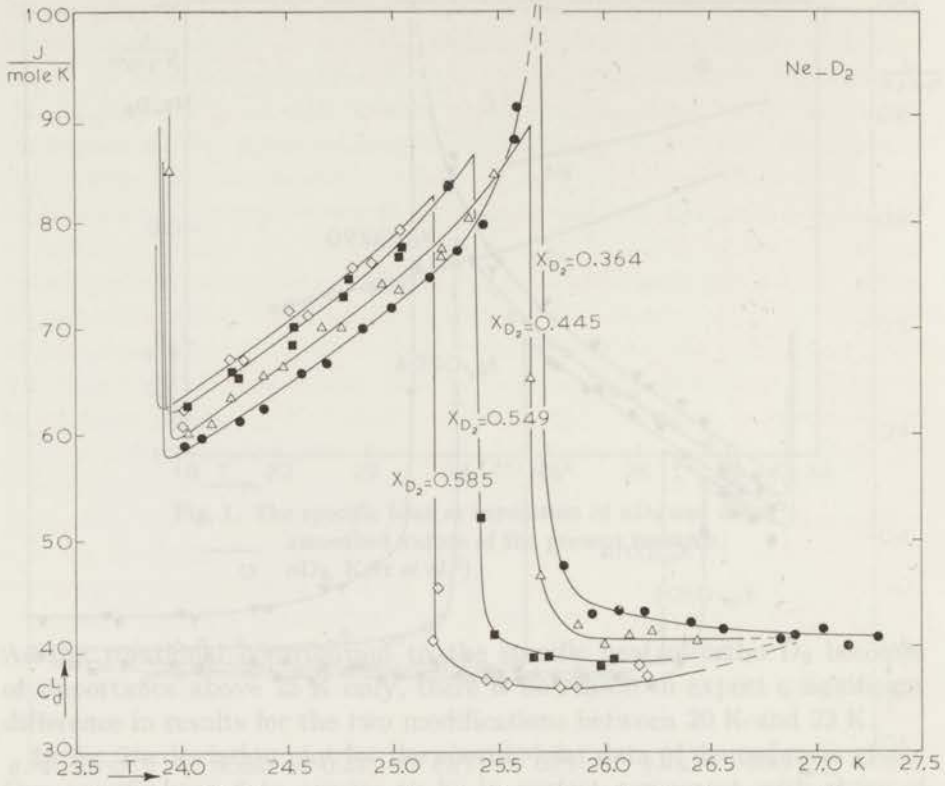


Fig. 4. Specific heat at saturation for the system Ne–$D_2$, for compositions $0.3 < x_{D_2} < 0.7$.

when the separated mixture becomes homogeneous. In table II the values of $T_M$ and $T_{PS}$ are listed. The tabulated composition values are the average liquid compositions over the whole temperature range of the measurements. The maximum variation of the liquid composition during a run was found to be 0.0002 only.

In fig. 6 a comparison is made with the results of earlier experiments. As can be seen, the phase diagram from the present experiment agrees fairly well with the phase diagram which we determined with a visual method (chapter I)[9]). There is a small difference in melting temperatures of about 0.06 K. In the visual method $T_M$ has been determined as the temperature at which the first crystals appeared in the liquid mixture. It is quite possible that such a method yields a somewhat too low value for the melting temperature. Furthermore a good agreement is found with the results for the phase-separation curve obtained from the pressure-composition measurements of Streett[6]). In fig. 7 his data in the phase-separation region are presented. A considerable discrepancy exists between the three above mentioned sources

TABLE I

Smoothed values of the specific heat $c_\sigma^L$ for the system Ne–$D_2$ (J/mole K)

| $T$ (K) \ $x_{D_2}$ | 0.000 (Ne) | 0.105 | 0.114 | 0.157 | 0.204 | 0.290 | 0.364 | 0.445 | 0.549 | 0.585 | 0.705 | 0.715 | 0.730 | 0.771 | 1.000 ($D_2$) |
|---|---|---|---|---|---|---|---|---|---|---|---|---|---|---|---|
| 24.0 | | 51.7 | 52.2 | 53.2 | 54.5 | 56.2 | 58.3 | 59.8 | 62.6 | 63.8 | 66.4 | 67.0 | 67.4 | 31.1 | 27.0 |
| 24.2 | | 53.7 | 54.4 | 55.4 | 57.1 | 58.9 | 60.8 | 62.6 | 65.2 | 66.3 | 68.7 | 69.8 | 31.9 | 31.2 | 27.2 |
| 24.4 | | 38.4 | 56.9 | 58.0 | 59.7 | 61.7 | 63.4 | 65.5 | 68.0 | 69.2 | 36.0 | 32.5 | 31.6 | 31.2 | 27.4 |
| 24.6 | (35.1)* | 36.6 | 37.8 | 60.7 | 62.4 | 64.5 | 66.1 | 68.3 | 70.9 | 72.2 | 32.9 | 32.6 | 31.7 | 31.2 | 27.6 |
| 24.8 | (35.3) | 36.6 | 37.4 | 63.5 | 65.2 | 67.4 | 69.1 | 71.3 | 73.9 | 75.4 | 33.0 | 32.7 | 31.8 | 31.4 | 27.8 |
| 25.0 | (35.5) | 36.7 | 37.4 | 66.5 | 68.2 | 70.4 | 72.2 | 74.5 | 77.5 | 78.8 | 33.1 | 32.8 | 31.9 | 31.6 | 28.2 |
| 25.2 | (35.7) | 36.8 | 37.4 | 38.0 | 71.9 | 74.4 | 75.5 | 77.9 | 81.8 | 40.6 | 33.2 | 32.9 | 32.0 | 31.8 | 28.3 |
| 25.4 | (35.9) | 36.8 | 37.5 | 38.0 | 76.5 | 80.0 | 80.2 | 82.1 | 66.0 | 37.2 | 33.4 | 33.0 | 32.2 | 31.9 | 28.5 |
| 25.6 | (36.1) | 36.9 | 37.5 | 38.0 | 41.8 | (91.6) | 90.8 | 87.7 | 39.9 | 36.3 | 33.6 | 33.2 | 32.4 | 32.1 | 28.8 |
| 25.8 | (36.3) | 37.0 | 37.5 | 38.1 | 40.8 | 48.4 | 47.3 | 42.1 | 39.0 | 36.0 | 33.8 | 33.5 | 32.5 | 32.3 | 29.0 |
| 26.0 | 36.4 | 37.0 | 37.6 | 38.1 | 40.2 | 46.0 | 43.6 | 40.7 | 38.6 | 36.2 | 34.0 | 33.7 | 32.7 | 32.5 | 29.2 |
| 26.2 | 36.6 | 37.1 | 37.6 | 38.1 | 40.0 | 44.4 | 42.7 | 40.7 | 38.6 | 36.4 | (34.2) | (33.9) | 32.9 | 32.7 | 29.5 |
| 26.4 | 36.8 | 37.1 | 37.7 | 38.2 | 40.0 | 43.6 | 42.1 | 40.7 | 38.9 | 37.2 | (34.4) | (34.1) | 33.1 | 32.9 | 29.7 |
| 26.6 | 37.0 | 37.2 | 37.7 | 38.3 | 39.9 | 43.2 | 41.6 | 40.8 | (39.4) | (38.0) | (34.6) | (34.4) | 33.3 | 33.1 | 30.0 |
| 26.8 | 37.2 | 37.3 | 37.8 | 38.4 | 39.9 | 42.9 | 41.3 | (40.8) | (39.9) | (39.2) | (34.8) | (34.6) | 33.5 | 33.3 | 30.3 |
| 27.0 | 37.4 | 37.4 | 37.9 | 38.6 | 39.9 | 42.8 | 41.1 | (40.8) | (40.4) | (40.2) | (35.0) | (34.8) | 33.8 | 33.6 | 30.5 |
| 27.2 | 37.5 | (37.6) | 38.0 | 38.7 | 39.9 | 42.8 | 41.0 | | | | | | 33.9 | 33.8 | 30.8 |
| 27.4 | 37.7 | (37.7) | 38.1 | 38.9 | (40.0) | 42.9 | 41.1 | | | | | | 34.2 | 34.2 | 31.1 |

* The brackets indicate extrapolated values.

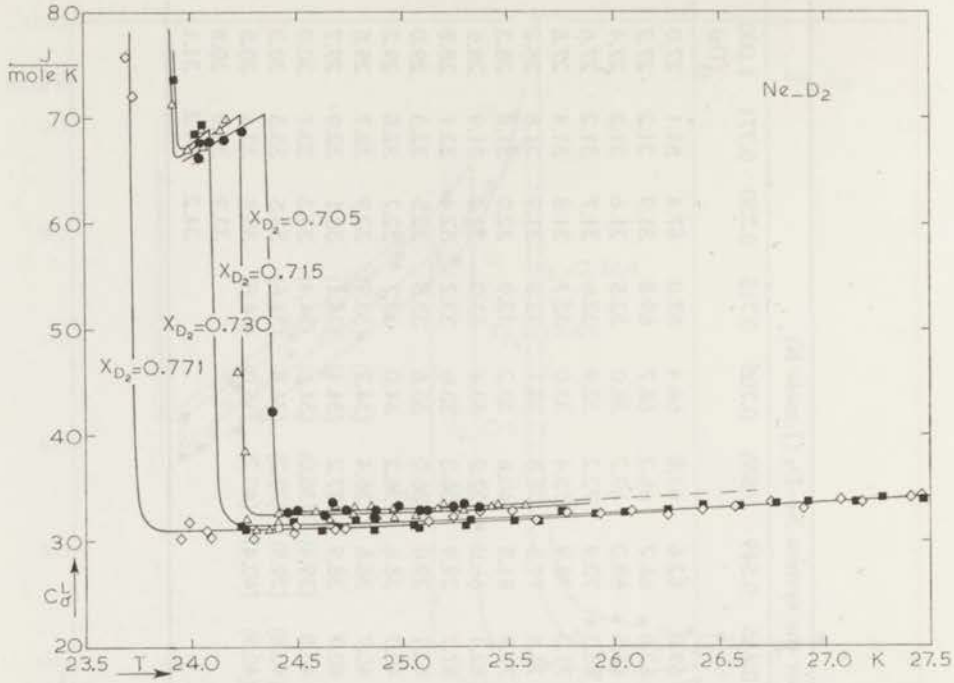


Fig. 5. Specific heat at saturation for the system Ne–$D_2$, for compositions $0.7 < x_{D_2}$.

TABLE II

| Transition temperatures | | | | | |
|---|---|---|---|---|---|
| $x_{D_2}$ | $T_M$ (K) | $T_{PS}$ (K) | $x_{D_2}$ | $T_M$ (K) | $T_{PS}$ (K) |
| 0.105 | 23.86 | 24.31 | 0.549 | 23.86 | 25.38 |
| 0.114 | 23.89 | 24.50 | 0.585 | 23.85 | 25.19 |
| 0.157 | | 25.16 | 0.705 | 23.88 | 24.35 |
| 0.204 | 23.87 | 25.48 | 0.715 | 23.86 | 24.24 |
| 0.290 | 23.86 | 25.68 | 0.730 | | 24.09 |
| 0.364 | 23.86 | 25.70 | 0.771 | 23.70 | |
| 0.445 | 23.85 | 25.65 | | | |

and the results of Simon (see fig. 6), who measured a single isotherm at 24.56 K[10]).

The composition of the upper critical consolute point has been obtained from the intersection of the rectilinear diameter $\frac{1}{2}(x_l + x_u)$ with the phase-separation curve. In table III the experimental data for the critical consolute point are given.

In fig. 8 the specific heat in the phase-separation region $c_{\bar{x}}^{L}$, is plotted as a function of the average liquid composition. For temperatures up to 25 K

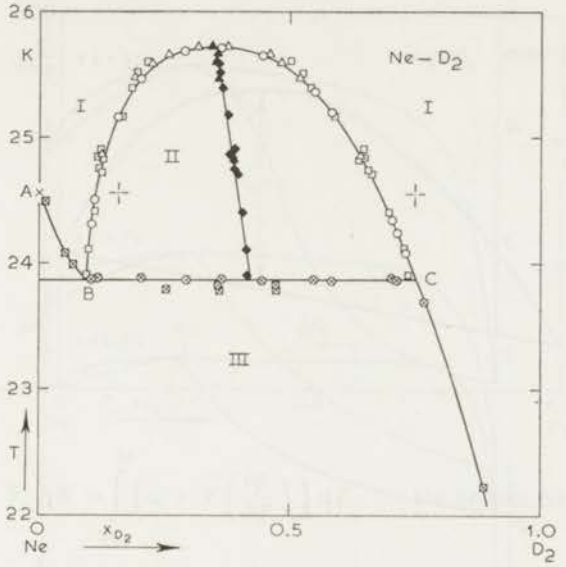


Fig. 6. The phase diagram at vapour-liquid equilibrium pressures for the system Ne–$D_2$.

○ phase-separation temperatures from the present experiment;
⊗ melting temperatures from the present experiment;
□ separation curve from visual observation[9]), ◆ $\frac{1}{2}(x_l + x_u)$;
⊠ melting points from visual observation[9]);
△ Streett[6]), ▲ $\frac{1}{2}(x_l + x_u)$;
⊣ Simon[10]);
× triple point Ne[11]);
—— $\frac{1}{2}(x_l + x_u)$ calculated from the separation curve according to the present experiment.

TABLE III

| The critical consolute point for the system Ne–n$D_2$ | | |
|---|---|---|
| | This experiment | Streett[6]) |
| $T_c$ | 25.71 ± 0.03 K | 25.74 ± 0.03 K |
| $x_c$ | 0.354 ± 0.002 | 0.347 ± 0.003 |
| $p_c$ | — | 2.07 ± 0.02 atm |

the data fit a straight line within 1%. This is in agreement with the leverage rule which gives rise to a linear relationship between $c_{\bar{x}}^{L}$ and the composition at constant temperature. Above 25 K the influence of the critical behaviour of the specific heat gives rise to a much larger scattering in the data.

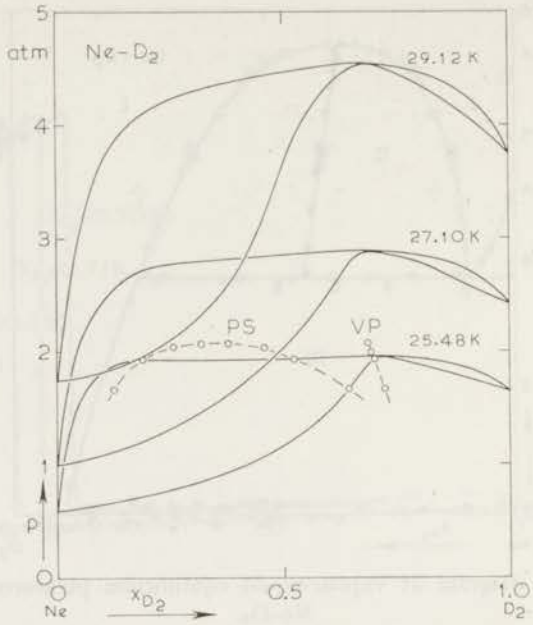


Fig. 7. Pressure-composition diagram for the system Ne–$D_2$ in the phase-separation region according to Streett[6]).

o ---- PS phase-separation curve

o ---- *VP* pressure-composition curve for the vapour phase in equilibrium with the separated liquid.

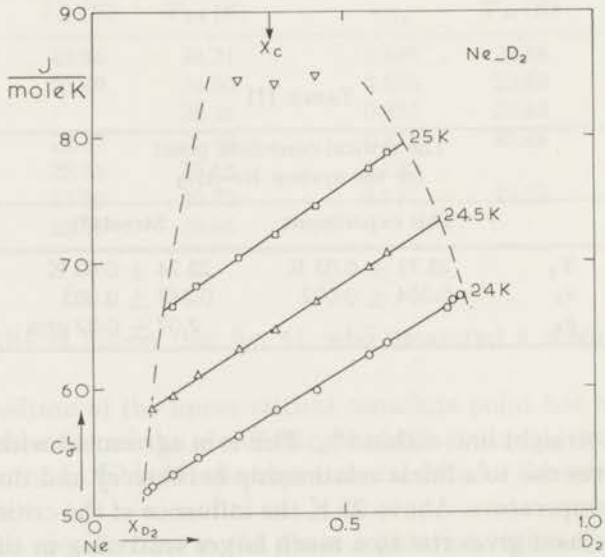


Fig. 8. Specific heat at saturation in the phase-separation region for the system Ne–$D_2$.

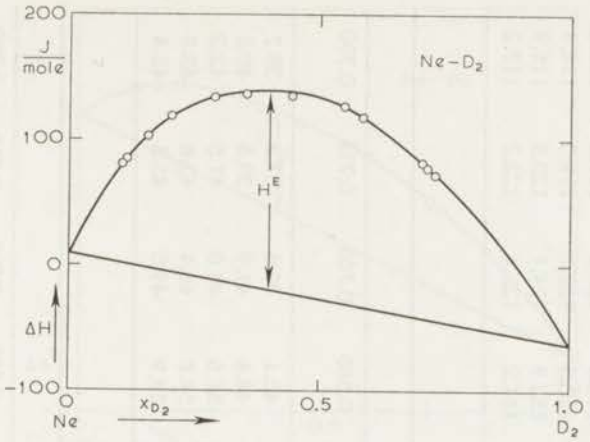


Fig. 9. $\Delta H = \int_{24}^{26} \left\{ c_\sigma + V \left( \frac{\partial p}{\partial T} \right)_\sigma \right\} dT$ for the system Ne–$D_2$.

5. *The excess functions.* For the calculation of the excess functions from the specific heat for the system Ne–$D_2$ we follow the same technique as has been used for the system Ne–$H_2$.

5a. The excess enthalpy. The difference in enthalpy between 24 K (just above $T_M$) and 26 K (just above $T_c$) at constant composition $\Delta H(\bar{x}, 26)$ has been calculated from the measured specific heat using the relation

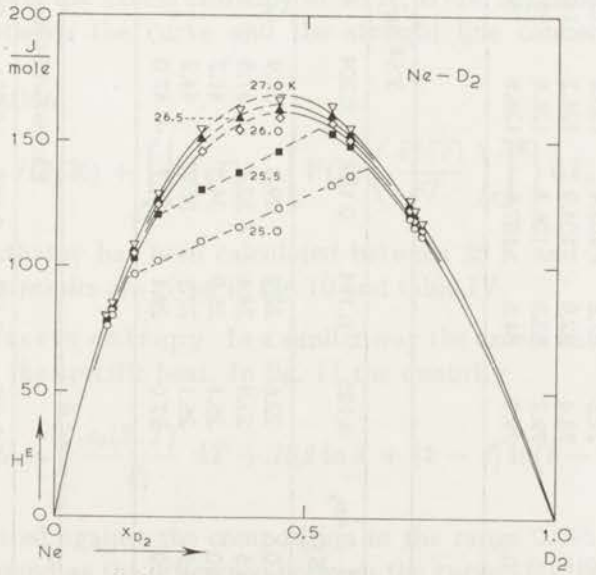


Fig. 10. The excess enthalpy for the system Ne–$D_2$ at different temperatures. The shape of the curves for $T > T_c$ near $x_c$ is discussed in section 6.

TABLE IV

Excess enthalpy for the system Ne–$D_2$ (J/mole)

| $T$ (K) \ $x_{D_2}$ | 0.105 | 0.114 | 0.157 | 0.204 | 0.290 | 0.364 | 0.445 | 0.549 | 0.585 | 0.705 | 0.715 | 0.730 |
|---|---|---|---|---|---|---|---|---|---|---|---|---|
| 25.0 | 76.4 | 80.4 | 96.9 | 102.0 | 110.0 | 116.0 | 123.6 | 132.6 | 136.3 | 119.4 | 116.0 | 112.6 |
| 25.5 | 77.5 | 81.8 | 103.4 | 120.8 | 130.8 | 137.9 | 146.0 | 153.4 | 148.0 | 120.8 | 117.5 | 113.8 |
| 26.0 | 78.4 | 82.9 | 104.9 | 124.2 | 145.9 | 154.6 | 159.2 | 157.0 | 150.3 | 122.3 | 119.0 | 114.9 |
| 26.5 | 79.2 | 83.8 | 106.3 | 126.6 | 151.0 | 159.1 | 162.8 | 160.2 | 152.9 | 124.1 | 120.5 | 115.9 |
| 27.0 | 79.9 | 84.5 | 107.5 | 128.8 | 155.0 | 162.7 | 166.5 | 164.0 | 154.2 | 126.4 | 122.2 | 117.2 |

TABLE V

$TS^E$ for the system Ne–$D_2$ (J/mole)

| $T$ (K) \ $x_{D_2}$ | 0.105 | 0.114 | 0.157 | 0.204 | 0.290 | 0.364 | 0.445 | 0.549 | 0.585 | 0.705 | 0.715 | 0.730 |
|---|---|---|---|---|---|---|---|---|---|---|---|---|
| 25.0 | 22.6 | 22.7 | 29.8 | 31.9 | 34.2 | 36.2 | 38.9 | 40.1 | 43.1 | 39.8 | 37.3 | 38.7 |
| 25.5 | 23.9 | 24.4 | 32.4 | 37.8 | 42.3 | 44.7 | 46.6 | 48.4 | 48.4 | 41.9 | 39.5 | 40.5 |
| 26.0 | 25.1 | 25.9 | 34.3 | 41.2 | 47.4 | 48.6 | 51.0 | 52.8 | 51.5 | 44.0 | 41.5 | 42.2 |
| 26.5 | 26.1 | 27.1 | 35.7 | 44.2 | 53.1 | 53.8 | 55.6 | 56.8 | 54.8 | 46.4 | 43.6 | 43.8 |
| 27.0 | 27.0 | 28.1 | 38.7 | 47.0 | 57.9 | 58.2 | 60.2 | 61.5 | 58.9 | 49.0 | 45.5 | 45.4 |

TABLE VI

Excess Gibbs function for the system Ne–$D_2$ (J/mole)

| $T$ (K) \ $x_{D_2}$ | 0.105 | 0.114 | 0.157 | 0.204 | 0.290 | 0.364 | 0.445 | 0.549 | 0.585 | 0.705 | 0.715 | 0.730 |
|---|---|---|---|---|---|---|---|---|---|---|---|---|
| 25.0 | 53.8 | 57.7 | 67.2 | 70.1 | 75.8 | 79.8 | 84.7 | 92.5 | 92.5 | 79.6 | 78.7 | 73.9 |
| 25.5 | 53.6 | 57.4 | 71.0 | 83.0 | 88.5 | 93.2 | 99.5 | 105.1 | 99.7 | 78.9 | 78.0 | 73.3 |
| 26.0 | 53.3 | 57.0 | 70.6 | 83.0 | 98.5 | 106.0 | 108.2 | 104.2 | 98.8 | 78.2 | 77.5 | 72.6 |
| 26.5 | 53.1 | 56.7 | 70.6 | 82.4 | 97.8 | 105.2 | 107.2 | 103.4 | 98.0 | 77.7 | 76.9 | 72.1 |
| 27.0 | 52.9 | 55.8 | 68.8 | 81.8 | 97.1 | 104.5 | 106.3 | 102.5 | 95.3 | 77.4 | 76.7 | 71.8 |

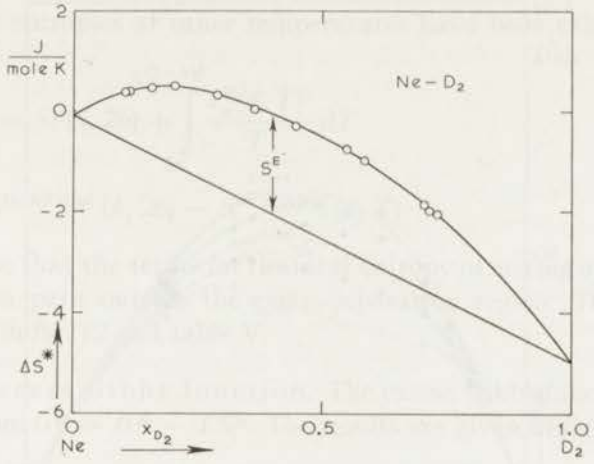


Fig. 11. $\Delta S^* = \int_{24}^{26} \frac{c_\sigma}{T}\,\mathrm{d}T + R\{x_{D_2} \ln x_{D_2} + (1 - x_{D_2}) \ln(1 - x_{D_2})\}$

for the system Ne–$D_2$.

$$\Delta H(\bar{x}, 26) = \int_{24}^{26} \left\{ c_\sigma(\bar{x}, T) + V(\bar{x}, T) \left( \frac{\partial p(\bar{x}, T)}{\partial T} \right)_\sigma \right\} \mathrm{d}T. \tag{2}$$

In fig. 9 the calculated values of $\Delta H(\bar{x}, 26)$ have been plotted as a function of composition in the range $0.095 \leq \bar{x} \leq 0.755$. Extrapolating this curve to $x = 0$ and $x = 1$, the excess enthalpy at 26 K, $H^E(\bar{x}, 26)$ is obtained as the difference between the curve and the straight line connecting the end points.

From the relation

$$H^E(T) = H^E(26) + \int_{24}^{T} \left\{ c_\sigma^E(T) + \left[ V(T) \left( \frac{\partial p(T)}{\partial T} \right)_\sigma \right]^E \right\} \mathrm{d}T, \tag{3}$$

the excess enthalpy has been calculated between 25 K and 27 K at 0.5 K intervals. The results are given in fig. 10 and table IV.

5b. The excess entropy. In a similar way the excess entropy has been derived from the specific heat. In fig. 11 the quantity

$$\Delta S^*(\bar{x}, 26) = \int_{24}^{26} \frac{c_\sigma(\bar{x}, T)}{T}\,\mathrm{d}T + R\{\bar{x} \ln \bar{x} + (1 - \bar{x}) \ln(1 - \bar{x})\} \tag{4}$$

has been plotted against the composition in the range $0.095 \leq \bar{x} \leq 0.755$. $S^E(\bar{x}, 26)$ is found as the difference between the curve and the straight line connecting the values of $\Delta S^*$ at $x = 0$ and $x = 1$.

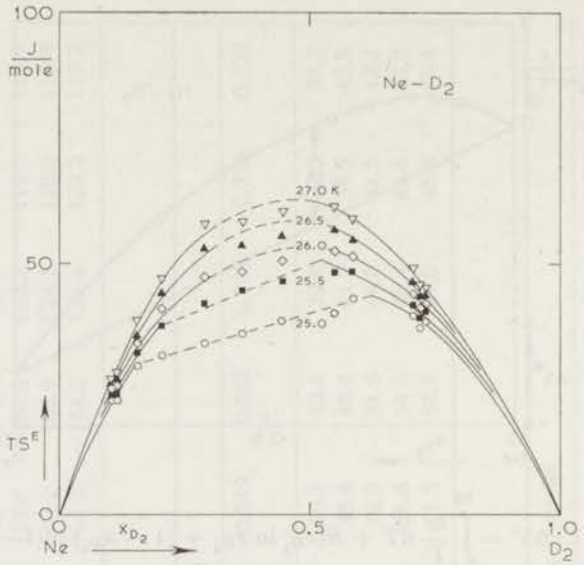


Fig. 12. $TS^{E}$ for the system Ne–$D_2$ at different temperatures. The shape of the curve for $T > T_c$ near $x_c$ is discussed in section 6.

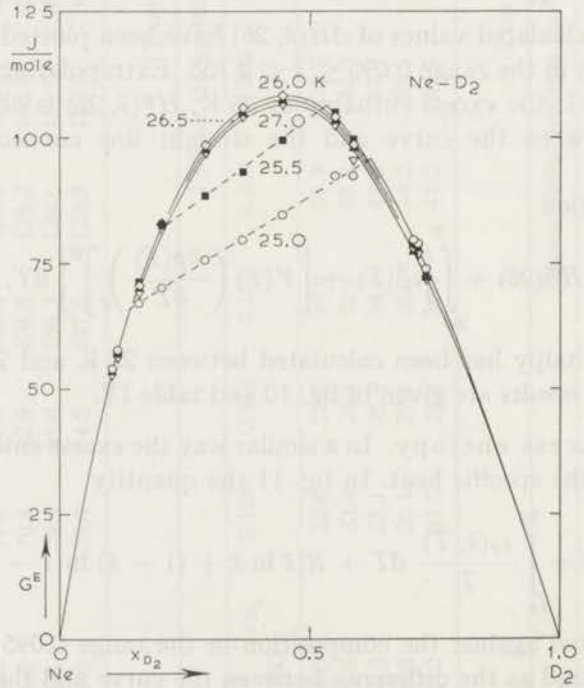


Fig. 13. The excess Gibbs function for the system Ne–$D_2$ at different temperatures.

The excess entropies at other temperatures have been calculated from:

$$S^{E}(\bar{x}, T) = S^{E}(\bar{x}, 26) + \int_{26}^{T} \frac{c_{\sigma}^{E}(\bar{x}, T)}{T} \, dT$$
$$+ S^{\text{id. mixing}}(\bar{x}, 26) - S^{\text{id. mixing}}(\bar{x}, T). \quad (5)$$

We emphasize that the terms for the ideal entropy of mixing only cancel for an integration path outside the phase-separation region. The results for $S^{E}$ are given in fig. 12 and table V.

5c. The excess Gibbs function. The excess Gibbs function has been calculated from $G^{E} = H^{E} - TS^{E}$. The results are given in fig. 13 and table VI.

We may note that the thermodynamic excess functions are extracted from the specific-heat measurements of mixtures with composition $\bar{x}$ in the interval $x_l(T_M) < \bar{x} < x_u(T_M)$. Since for the system Ne–$D_2$ the maximum difference between $x_u$ and $x_l$ is about 0.65 at the melting temperature $T_M$, the extrapolation to $x = 0$ and $x = 1$ covers a rather large composition interval, which introduces an extra inaccuracy in the derived excess functions.

In fig. 14 a representation is given of $H^{E}$, $TS^{E}$ and $G^{E}$ at 26 K together

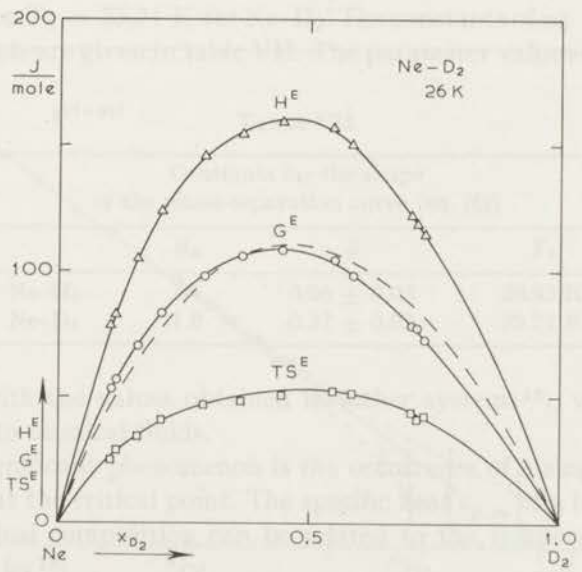


Fig. 14. The excess functions $H^{E}$, $TS^{E}$ and $G^{E}$ at 26 K.
⊔ $TS^{E}$, ○ $G^{E}$, △ $H^{E}$,
--- $G^{E}$ calculated from the data of Streett[6]).

with $G^E$ calculated from the pressure-composition measurements of Streett[6]). There is a good agreement between the values of $G^E$ obtained from both experiments. From the pressure-composition isotherms at different temperatures it is also possible to obtain the excess entropy, using the relation $S^E = -dG^E/dT$. From such a calculation based on the data of Streett not very accurate values for $S^E$ are obtained. Within the limits of accuracy, however, these $S^E$ values are in agreement with our results.

6. *Critical phenomena.* From the study of the critical behaviour of many systems it has been found that the shape of the coexistence curve of a two-phase system can be described by the following relation[12]):

$$x_u - x_l = B_x \{(T_c - T)/T_c\}^\beta \qquad (6)$$

where $x_u - x_l$ is the mole fraction difference between the two liquid phases at temperature $T$, and $B_x$ and $\beta$ are constants. In the case of the liquid–vapour system a similar relation holds for the difference in density between the coexisting liquid and gas phase. In both cases $\beta$ has approximately the value $\frac{1}{3}$.

In order to determine $B_x$ and $\beta$ for our phase-separation curves the difference in mole fraction between upper and lower phase has been plotted as a function of $(T_c - T)/T_c$ on a double log scale for the system Ne–$H_2$ in fig. 15 and for the system Ne–$D_2$ in fig. 16. The value of the critical

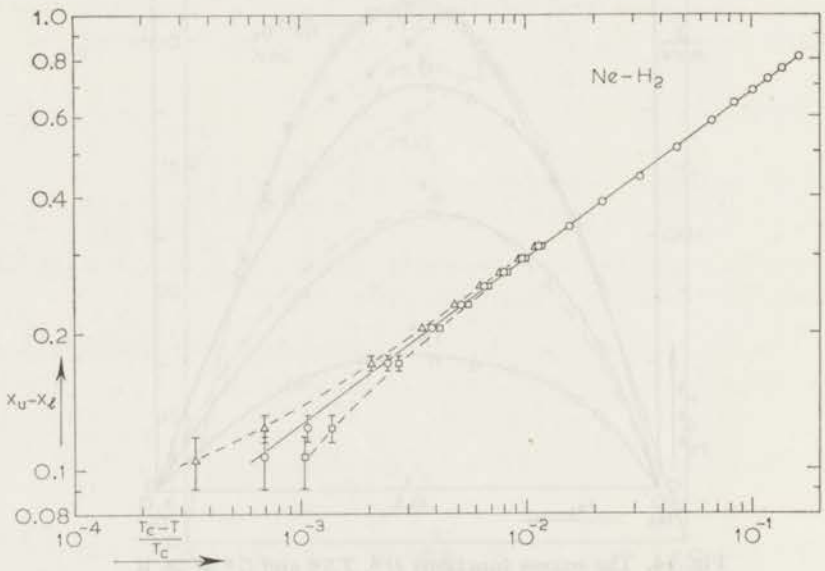


Fig. 15. The shape of the phase-separation curve for the system Ne–$H_2$.
△ $T_c = 28.92$ K, ○ $T_c = 28.93$ K, □ $T_c = 28.94$ K.

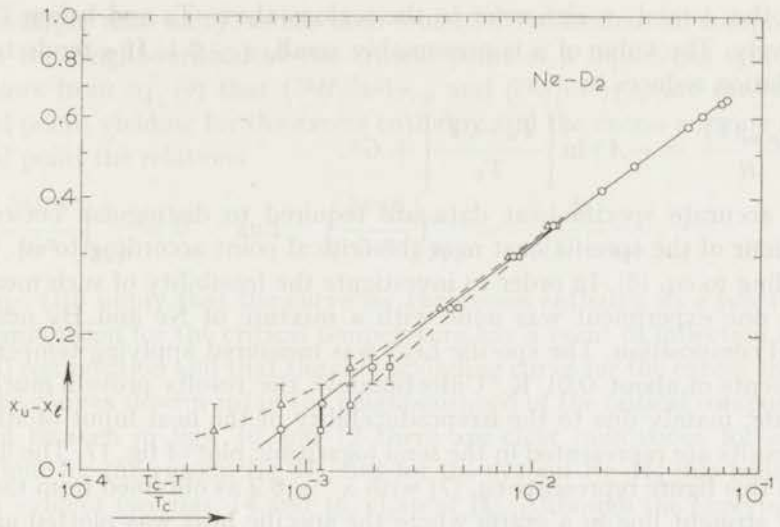


Fig. 16. The shape of the phase-separation curve for the system Ne–$D_2$.
△ $T_c = 25.70$ K, ○ $T_c = 25.71$ K, □ $T_c = 25.72$ K.

temperature is determined from the specific-heat measurements with an accuracy of $\pm 0.03$ K. We therefore plotted the mole-fraction difference for three values of $T_c$: for Ne–$H_2$ 28.92 K, 28.93 K and 28.94 K and for Ne–$D_2$ 25.70 K, 25.71 K and 25.72 K. Apparently the points fit a straight line best over the whole temperature range for $T_c = 28.93$ K for the system Ne–$H_2$ and for $T_c = 25.71$ K for Ne–$D_2$. The constants of eq. (6) determined from these plots are given in table VII. The parameter values obtained agree

TABLE VII

Constants for the shape of the phase-separation curve [eq. (6)]

| | $B_x$ | $\beta$ | $T_c$ |
|---|---|---|---|
| Ne–$H_2$ | 1.6 | $0.36 \pm 0.03$ | 28.93 K |
| Ne–$D_2$ | 1.8 | $0.37 \pm 0.03$ | 25.71 K |

rather well with the values obtained for other systems[12]), which however mainly refer to classical fluids.

Another significant phenomenon is the occurrence of a singularity in the specific heat at the critical point. The specific heat $c_{p,x_c}$ of a binary mixture with the critical composition can be related to the temperature near the critical point by[13])

$$\frac{c_{p,x_c}(T)}{R} = A^{\pm}\left\{\frac{|(T_c - T)/T_c|^{-\alpha^{\pm}} - 1}{\alpha^{\pm}}\right\} + G^{\pm}, \qquad (7)$$

where the + and − sign refer to the regions above $T_c$ and below $T_c$, respectively. The value of $\alpha$ is presumably small, $\alpha \leq 0.1$. If $\alpha$ tends to zero the relation reduces to

$$\frac{c_{p,x_c}(T)}{R} = -A^{\pm} \ln \left| \frac{T_c - T}{T_c} \right| + G^{\pm}. \tag{8}$$

Quite accurate specific-heat data are required to distinguish between a behaviour of the specific heat near the critical point according to eq. (7) or according to eq. (8). In order to investigate the feasibility of such measurements one experiment was done with a mixture of Ne and $H_2$ near the critical composition. The specific heat was measured applying temperature increments of about 0.01 K. Unfortunately the results proved much less accurate, mainly due to the irreproducebility of the heat input of stirring. The results are represented in the semi logaritmic plot of fig. 17. The dashed line in this figure represents eq. (7) with $\alpha^- = 0.2$ as obtained from the best fitting straight line in a graph where the specific heat was plotted against $\{(T_c - T)/T_c\}^{-0.2}$. It is clear from fig. 17 that significant information about the value of $\alpha^-$ can only be extracted from the specific-heat data if the measurements extend to $T_c - T < 0.02$ K. This requires a measuring accuracy which is an order of magnitude better than that obtained with the present apparatus, which was designed to measure the specific heat over a wide temperature range.

We may finally note that the critical coefficient $\gamma^+$ in the case of a binary mixture appears in the relation

$$\left(\frac{\partial^2 G}{\partial x^2}\right)_{T,p} = C\left(\frac{T - T_c}{T_c}\right)^{\gamma^+}, \qquad T > T_c. \tag{9}$$

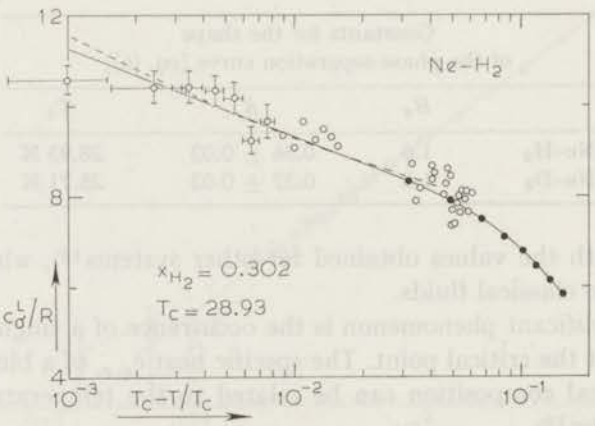


Fig. 17. The specific heat of a mixture with the critical composition for temperatures below $T_c$. The dashed line has been calculated according to the power law with $\alpha^- = 0.2$.
● smoothed values from fig. 11, chapter II.

If $\gamma^+$ is larger than unity, as has been found for the isothermal compressibility in the neighbourhood of the critical point of a liquid–gas system[14]), it follows from eq. (9) that $(\partial^2 H/\partial x^2)_{T,p}$ and $(\partial^2 S/\partial x^2)_{T,p}$ are zero at the critical point, yielding for the excess enthalpy and the excess entropy at the critical point the relations

$$\left(\frac{\partial^2 H^E}{\partial x^2}\right)_{T,p} = 0 \quad \text{and} \quad \left(\frac{\partial^2 S^E}{\partial x^2}\right)_{T,p} = \frac{R}{x_c(1-x_c)}. \tag{10}$$

The eqs. (10) imply that the curve for the excess enthalpy as a function of the composition for the critical temperature has a point of inflection at the critical composition and that the corresponding curve for the excess entropy must be convex downward in the neighbourhood of the critical composition. As can be seen in figs. 10 and 12 there are clear indications for such a behaviour for the system Ne–$D_2$, but for the system Ne–$H_2$ this behaviour is less evident (see figs. 14 and 16, chapter II). Although the experimental data refer to the saturated vapour pressure instead of constant pressure, the variation of the pressure as a function of composition near the critical point is too small to have a significant influence on the shape of the curve.

7. *Conclusions.* In order to get an understanding of the main features of the excess functions in isotopic mixtures of quantum liquids we follow the approach developed by Prigogine and his group[2]). In this approach each particle is assumed to move in a cell constituted by its neighbours. For large quantum effects ($\Lambda^* \gg 1$) the zero-point volume is much larger than the classical volume at 0 K. In this situation the smoothed potential model[15]) may be introduced, which implies that each particle moves in a square-well potential. In this model the reduced zero-point energy $E_0^* = E_0/\varepsilon$ is proportional to $\Lambda^{*2}$. The total reduced energy at 0 K then can be written as the sum of the lattice energy and the zero-point energy, *i.e.*:

$$E^*_{T=0} = E^*_{\text{latt.}}(V^*) + \Lambda^{*2}\Psi(V^*), \tag{11}$$

where $E^*_{\text{latt.}}$ and $\Psi$ are functions of the reduced volume $V^* = V/N\sigma^3$. At vanishing external pressure the relation $-\partial E^*_{T=0}/\partial V^* = 0$ yields the equation of state:

$$V^* = V^*(\Lambda^{*2}). \tag{12}$$

Substituting eq. (12) into eq. (11) the reduced energy at 0 K can be expressed as a function of $\Lambda^{*2}$ alone:

$$E^*_{T=0} = E^*_{T=0}(\Lambda^{*2}). \tag{13}$$

If one now accepts that the properties of an isotopic mixture are characterized by an average value of $\Lambda^{*2}$ defined as:

$$\langle\Lambda^{*2}\rangle = x\Lambda_1^{*2} + (1-x)\Lambda_2^{*2}, \tag{14}$$

the excess energy at 0 K can be determined from

$$E^{*E}_{T=0} = E^{*}_{T=0}(\langle \Lambda^{*2} \rangle) - \{xE^{*}_{T=0}(\Lambda_1^{*2}) + (1-x)\, E^{*}_{T=0}(\Lambda_2^{*2})\}. \qquad (15)$$

For nonzero temperatures this method may still be used if the thermal energy remains small compared to the zero-point energy. One can neglect the influence of the term $pV^E$, which implies that one can take $H^E = E^E$.

As neon and the hydrogen isotopes may be regarded as isotopes in the sense that the potential parameters are nearly equal one expects that this scheme to calculate $H^E$ may also be applied here. Therefore we have plotted in fig. 18 the values of $E^*$ as a function of $\Lambda^{*2}$. The reduced energy has been calculated at two different reduced temperatures $T^* = kT/\varepsilon$, from the experimental data of the heat of evaporation and the vapour pressure of neon[3]) and the hydrogen isotopes[4,5]), using the ideal gas as a reference state. The two curves in fig. 18 correspond with $T = 26$ K and $T = 29$ K, where the small differences in $T^*$ arising from the differences in $\varepsilon/k$ for the substances, have been neglected. The values of $H^E$ obtained from these graphs for the systems Ne–$H_2$ and Ne–$D_2$ are given in table VIII, together with the experimental results. A similar comparison is made with the values

TABLE VIII

Excess quantities for equi-molar mixtures of different binary systems

| | | Experimental | | Reduced energy as a function of $\Lambda^{*2}$ | Expansion–compression method |
|---|---|---|---|---|---|
| | $T$ (K) | $H^E$ (J/mole) | $G^E$ (J/mole) | $H^E$ (J/mole) | $G^E$ (J/mole) |
| Ne–$H_2$ | 29 | 200 | 125 | 210 | 90 |
| Ne–$D_2$ | 26 | 160 | 110 | 100 | 60 |
| $H_2$–$D_2$ | 20 | 12.2[16]) | 7.2[16,17]) | 40 | 9 |
| $H_2$–HD | 20 | 5 [16]) | 2.6[16,17]) | 25 | 2.4 |
| HD–$D_2$ | 20 | 3.7[16]) | — | 12 | 2.1 |

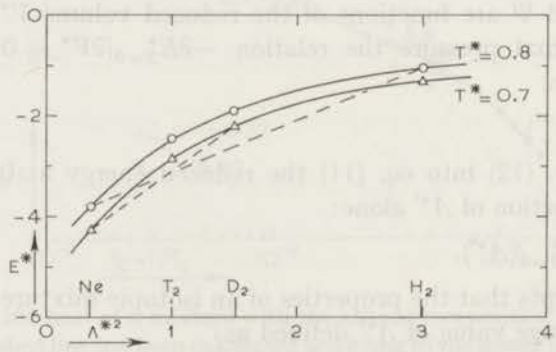


Fig. 18. The reduced energy as a function of $\Lambda^{*2}$.

of $H^E$ for the mixtures of the hydrogen isotopes as have been measured by Knaap *et al.*[16]). Although the theoretical value of $H^E$ for the system Ne–$H_2$ is in good agreement with the experimental result, the calculated value for the system Ne–$D_2$ is much too low and for mixtures of the hydrogen isotopes much too high. In this method the determination of the excess enthalpy is strongly dependent on the curvature of the reduced energy *versus* $\Lambda^{*2}$ curve. The main objection to this method is the oversimplification introduced with the smoothed potential model, which implies the quadratic dependence of the reduced energy on $\Lambda^*$. Moreover it is questionable whether this model, valid for large values of $\Lambda^*$, is applicable to these systems.

Starting from the basic assumption of Prigogine's theory, Simon and Bellemans[18]) developed an improved method to calculate the excess quantities. The idea of this method is that the difference in molar volume between two isotopes is due to the difference in zero-point energy only, and hence the two liquids are expected to mix almost ideally when brought to the same molar volume. Considering for example the system Ne–$H_2$, the two components can be brought to the same volume in a hypothetical experiment if the lighter isotope (volume $V^0_{H_2}$, pressure $p^0_{H_2}$) is isothermally compressed to a volume $V^M$ and pressure $p'_{H_2}$, while the heavier isotope ($V^0_{Ne}$, $p^0_{Ne}$) is expanded to the same volume $V^M$ by applying a negative pressure $p'_{Ne}$ (see

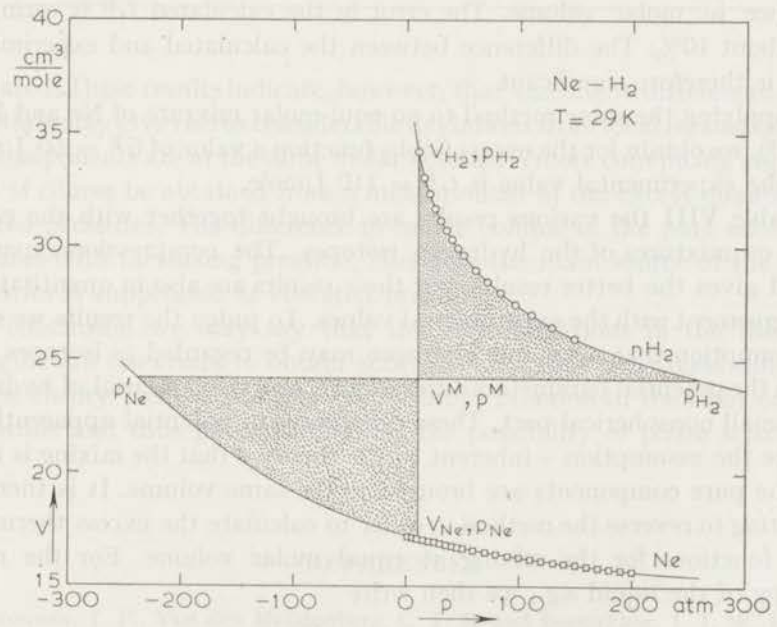


Fig. 19. Diagram for the calculation of $F^E$.
○ molar volume of $H_2$ as a function of pressure[19]).
□ molar volume of Ne as a function of pressure[3]).

fig. 19). The pressures $p'_{H_2}$ and $p'_{Ne}$ have to be taken in such a way that the total pressure after mixing equals the pressure $p^M$ of the mixture, *i.e.*:

$$x p'_{H_2} + (1 - x)\, p'_{Ne} = p^M. \tag{16}$$

From this relation and the equations of state for neon and hydrogen the value of $V^M$ can be determined.

If it is assumed that the two components mix ideally, once they are brought to the same volume the total excess free energy is given by the sum of the compression and expansion work:

$$F^E = -x \int_{V^0_{H2}}^{V^M} p \, dV - (1 - x) \int_{V^0_{Ne}}^{V^M} p \, dV \tag{17}$$

One can easely show that this method always leads to a positive $F^E$, and since the influence of $pV^E$ is negligibly small compared to the excess free energy, $F^E$ is almost equal to $G^E$. Once $G^E$ is known, $S^E$ and $H^E$ can be calculated from $S^E = -(\partial G^E/\partial T)_p$ and $H^E = G^E + TS^E$. For an equi-molar mixture of Ne–$H_2$ this method gives at 29 K a value $F^E \approx G^E = 90$ J/mole, while the experiments yield a value of $G^E = 125$ J/mole.

As can be seen from fig. 19 the isotherm of hydrogen[19]) has to be extrapolated to a rather high pressure and the isotherm of neon[3]) has to be extrapolated to a rather large negative pressure, because of the large difference in molar volume. The error in the calculated $G^E$ is estimated to be about 10%. The difference between the calculated and experimental values is therefore significant.

By applying the same method to an equi-molar mixture of Ne and $D_2$ at 26 K[3,5]), we obtain for the excess Gibbs function a value of $G^E = 60$ J/mole, while the experimental value is $G^E = 110$ J/mole.

In table VIII the various results are brought together with the earlier results on mixtures of the hydrogen isotopes. The compression-expansion method gives the better results, but these results are also in quantitatively poor agreement with the experimental values. To judge the results we recall the assumption that neon and hydrogen may be regarded as isotopes even though the potential parameters differ slightly and the potential of hydrogen has a small nonspherical part. These differences in potential apparently invalidate the assumption – inherent to the theory – that the mixing is ideal, once the pure components are brought to the same volume. It is therefore interesting to reverse the method in order to calculate the excess thermodynamic functions for the mixing at equal molar volume. For the molar enthalpy of the liquid *e.g.*, we then write

$$H = x H^0_1(p'_{H_2}) + (1 - x)\, H^0_2(p'_{Ne}) + H^{E'}, \tag{18}$$

where $p'_{H_2}$ and $p'_{Ne}$ are the pressures obtained from the graph in fig. 19.

However, the same final state of the mixture is also obtained by mixing the pure components at their saturated vapour pressure, yielding for the enthalpy

$$H = xH_1^0(p_{H_2}^0) + (1 - x)\, H_2^0(p_{Ne}^0) + H^E. \qquad (19)$$

Substracting eq. (19) from eq. (18) we obtain for an equi-molar mixture

$$H^{E'} = H^E + \tfrac{1}{2}\{H_1^0(p_{H_2}^0) - H_1^0(p'_{H_2})\} + \tfrac{1}{2}\{H_2^0(p_{Ne}^0) - H_2^0(p'_{Ne})\}. \qquad (20)$$

The value of $H^E$ is known from the present experiment and the second and third terms on the right-hand side of eq. (20) can be evaluated by extrapolating the known enthalpy *versus* pressure data of the pure components[3,4,5]). The results of such calculations of $H^{E'}$ and $TS^{E'}$ for the system Ne–$H_2$ at 29 K and for the system Ne–$D_2$ at 26 K are given in table IX, together with the values of $G^{E'}$ derived from the $p$–$V$ diagram. We emphasize that this type of calculation is rather crude and that the indicated accuracy is only roughly

TABLE IX

The excess functions for mixing at equal molar volume

| | $T$ (K) | $H^{E'}$ (J/mole) | $TS^{E'}$ (J/mole) | $G^{E'}$ (J/mole) |
|---|---|---|---|---|
| Ne–$D_2$ | 26 | 65 ± 20 | 15 ± 20 | 50 ± 10 |
| Ne–$H_2$ | 29 | 100 ± 20 | 70 ± 20 | 30 ± 10 |

estimated. These results indicate, however, that the slight differences in the potentials may give rise to considerable deviations from ideal mixing once the pure components are at the same molar volume. A more convincing argument could of course be obtained from a measurement of the excess quantities at elevated pressures. The difference in molar volume of the pure substances decreases with increasing pressure, therefore the main source of the excess quantities is suppressed at elevated pressures.

In conclusion we may say that the approximations in the theory of Prigogine are too crude to obtain accurate values for the excess functions, but the theory yields a positive excess Gibbs function in the right order of magnitude and thus properly predicts the possibility of phase separation.

REFERENCES


1) Brouwer, J. P., Van den Meijdenberg, C. J. N. and Beenakker, J. J. M., Physica (1970), to be published (Commun. Kamerlingh Onnes Lab., Leiden No. 380*a*).
2) Prigogine, I., The Molecular theory of solutions (North-Holland Publishing Cy. Amsterdam, 1957).

3) McCarthy, R. D. and Stewart, R. B., Nat. Bur. Stand. (U.S.) Rept. 8726.
4) Woolley, H. W., Scott, R. B. and Brickwedde, F. B., J. Res. Nat. Bur. Stand. **41** (1948) 379.
5) Prydz, R., Nat. Bur. Stand. (U.S.) Rept. 9276.
6) Streett, W. B., Proc. intern. cryog. Eng. Conf., 2nd, Brighton, U.K., (1968) 260.
7) Kerr, E. C., Rifkin, E. B., Johnston, H. L. and Clarke, J. T., J. Amer. Chem. Soc. **73** (1951) 282.
8) Osborne, N. S., Steinson, H. F., Sligh, T. S. and Cragoe, C. S., Sci. Papers Nat. Bur. Stand. (U.S.) **20** (1925) 66.
9) Brouwer, J. P., Hermans, L. J. F., Knaap, H. F. P. and Beenakker, J. J. M., Physica **30** (1964) 1409 (Commun. Kamerlingh Onnes Lab., Leiden No. 339*b*).
10) Simon, M., Physica **29** (1963) 1079.
11) Grilly, E. R., Cryogenics **2** (1962) 226.
12) Heller, P., Rep. Progr. Phys. **30** (1967) 731.
13) Kadanoff, L. P., Götze, W., Hamblen, D., Hecht, R., Lewis, E. A. S., Palciauskas, V. V., Rayl, M., Swift, J., Aspnes, D. and Kane, J., Rev. mod. Phys. **39** (1967) 395.
14) Rowlinson, J. S., Proc. intern. Conf. on critical Phenomena, Washington, U.S., (1965), Nat. Bur. Stand. Misc. Publ. **273** (1966) 9.
15) Prigogine, I. and Mathot, V., J. chem. Phys. **20** (1952) 49.
16) Knaap, H. F. P., Van Heijningen, R. J. J., Korving, J. and Beenakker, J. J. M., Physica **28** (1962) 343 (Commun. Kamerlingh Onnes Lab., Leiden No. 333*b*).
17) Bellemans, A., Bull. Soc. Chim. Belg. **68** (1959) 270.
18) Simon, M. and Bellemans, A., Physica **26** (1960) 191.
19) Friedman, A. S. and Hilsenrath, J., Nat. Bur. Stand. (U.S.) Rept. 3163 and Rept. 3282.

# SAMENVATTING

In dit proefschrift worden onderzoekingen beschreven aan de fase-scheiding van de systemen Ne–$D_2$ en Ne–$H_2$ in de vloeibare toestand. Het doel van de experimenten is gegevens te verkrijgen over de invloed van quantum mechanische verschijnselen op de thermodynamische eigenschappen van mengsels. In de inleiding is uiteengezet dat mengsels van Ne en de waterstof isotopen zeer geschikt zijn voor een onderzoek naar de invloed van de nulpunts-energy op het gedrag van mengsels. Enerzijds bestaat er tussen neon en de waterstof isotopen een groot verschil in massa, anderzijds zijn de parameters van de intermoleculaire wisselwerking voor neon weinig verschillend van die voor waterstof en deuterium. De grote afwijkingen van ideale menging, zoals die zich manifesteren in de fase-scheiding zijn daarom voornamelijk het gevolg van het verschil in nulpunts-energie.

In hoofdstuk I worden de metingen beschreven aan de fase-scheiding van het systeem Ne–$D_2$. Met de toegepaste visuele onderzoekingsmethode is op eenvoudige en directe wijze de fase-scheidingskromme bepaald. In de hoofdstukken II en III worden respectievelijk de soortelijke warmte metingen aan de systemen Ne–$H_2$ en Ne–$D_2$ beschreven. De soortelijke warmte van de vloeistof in het ontmenggebied bevat een bijdrage die het gevolg is van de menging van de twee vloeistoffasen. Het is mogelijk uit de soortelijke warmte gegevens de exces enthalpie, de exces entropie en de exces Gibbs functie te bepalen. In een appendix bij hoofdstuk II wordt in detail de uitdrukking voor de warmte capaciteit van een vloeistof-dampsysteem bestaande uit twee componenten afgeleid, zoals die in hoofdstuk II is gebruikt. In hoofdstuk III wordt naast de soortelijke warmte metingen van het systeem Ne–$D_2$, aandacht besteed aan de verschijnselen die optreden in de buurt van het kritische punt. De kritische coëfficiënt $\beta$, die de vorm van de fase-

scheidings kromme beschrijft, is uit de meetresultaten berekend. De experimentele exces grootheden geven een duidelijke aanwijzing dat de kritische coëfficiënt $\gamma^+$ groter is dan 1. Een nauwkeurige bepaling van de coëfficiënt $\alpha$ valt buiten de mogelijkheden van dit onderzoek.

Tenslotte worden de experimentele resultaten van zowel het systeem Ne–$H_2$ als van het systeem Ne–$D_2$ vergeleken met de theorieën van Prigogine en medewerkers voor vloeibare mengsels van isotopen. De veronderstelling, dat de quasi-isotopen Ne–$H_2$ en Ne–$D_2$ ideaal mengen bij gelijk molair volume blijkt niet juist te zijn.

Teneinde te voldoen aan de wens van de Faculteit der Wiskunde en Natuurwetenschappen volgt hier een overzicht van mijn studie.

Na het beëindigen van de H.B.S.-B.-opleiding aan het Christelijk Lyceum „Zandvliet" te 's-Gravenhage begon ik in 1956 mijn studie aan de Rijksuniversiteit te Leiden. Het candidaatsexamen met de hoofdvakken natuurkunde en wiskunde en het bijvak scheikunde werd in 1960 afgelegd. Het doctoraalexamen experimentele natuurkunde met bijvak mechanica legde ik af in 1964. Sinds april 1961 ben ik werkzaam in de groep molecuulfysica van het Kamerlingh Onnes Laboratorium. De leiding van deze groep berustte aanvankelijk bij Prof. Dr. K. W. Taconis en is thans in handen van Prof. Dr. J. J. M. Beenakker. Veel experimentele ervaring deed ik op onder leiding van Dr. H. F. P. Knaap, in samenwerking met wie ook de experimenten in het eerste hoofdstuk beschreven, verricht werden.

Vanaf de cursus 1962–1963 heb ik op het practicum voor pre-candidaten geassisteerd. De onderzoekingen die in dit proefschrift beschreven zijn, werden verricht in samenwerking met achtereenvolgens de heren Drs. L. J. F. Hermans, Drs. W. M. van Beek, D. J. van den Bos, Drs. A. L. J. Burgmans, Drs. A. M. Vossepoel, K. W. Walstra en W. C. Turkenburg. Technische hulp werd verleend door de heren J. M. Verbeek en J. Turenhout, terwijl de heer C. le Pair immer klaar stond met zijn vloeibare waterstof. De heer B. Kret en zijn staf verzorgden de glazen apparatuur.

Veel profijt heb ik gehad van de discussie met Dr. H. F. P. Knaap die dit manuscript van critische opmerkingen voorzag. Erkentelijk ben ik Dr. V. G. Cooper voor het corrigeren van de engelse tekst. In het bijzonder wil ik mej. A. M. Aschoff bedanken, die het manuscript in getypte vorm bracht en de heer W. F. Tegelaar, die de tekeningen verzorgde.